

Ada Lovelace Workshop 2019, Siena, Italy



The iron spin transition

Identification and implications for mantle dynamics

Grace E. Shephard
grace.shephard@geo.uio.no



Centre for Earth Evolution and Dynamics (CEED)
University of Oslo, Norway

The iron spin transition

Identification and implications for mantle dynamics



Christine Houser



John Hernlund



Renata
Wenzkovitch



Reidar Trønnes



Juan
Valencia-Cardona

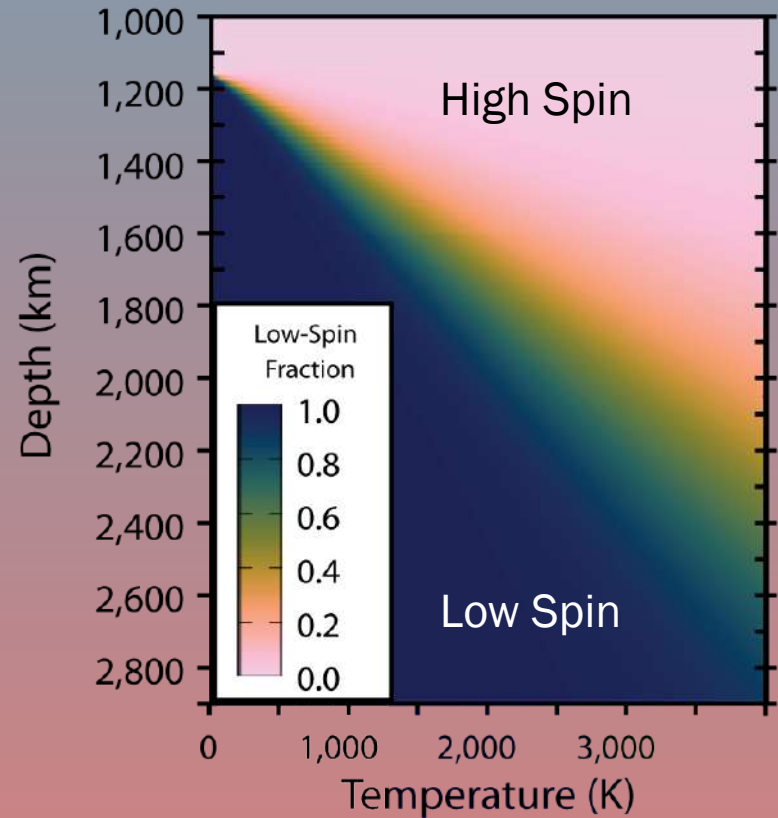


Aim of this study

- Ferropericlase ~20% lower mantle
- Iron in Fp undergoes a spin transition
- Experimentally proven but not readily apparent in seismic data

Why not

Are mineral physics predictions wrong ?
Seismic resolution poor ?
Is there not enough Fp?



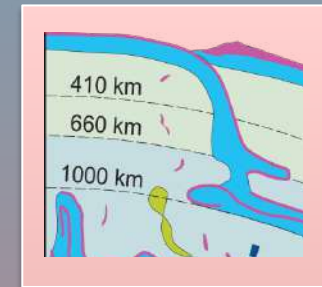
Aim of this study

Spin changes thermo-elastic properties and convective behaviour:

- Slabs

May stall, reorganise or avalanche

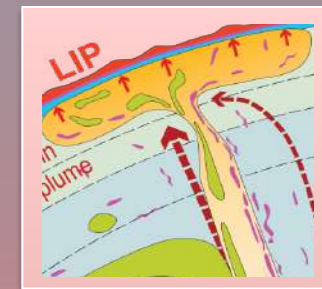
(e.g. Morra et al. 2010, Shahnas et al., 2011)



- Plumes

May enhance vigour, plume head dynamics

(e.g. Bower et al., 2009; Shahnas et al., 2011; Justo et al., 2015)



- LLSVPs

May enhance boundaries and stability, or not.

(e.g. Huang et al. 2015; Li et al., 2018)



Talk Overview

[1] Overview Mantle Structure and Composition

[2] Iron spin transition

- Mineral physics
- Seismology

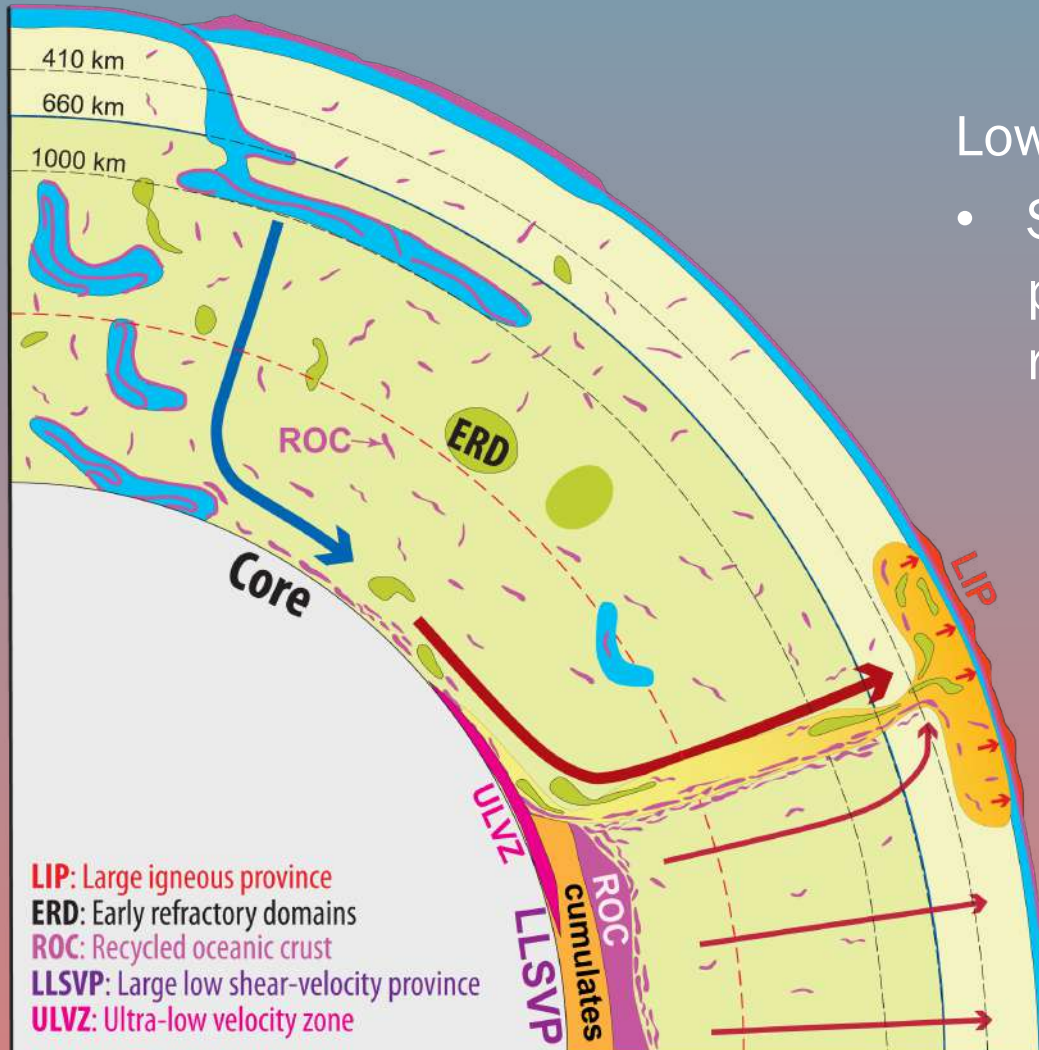
[3] Vote maps

[4] Geodynamic implications

- BEAMS structures

Mantle structure and composition

Structure of the mantle



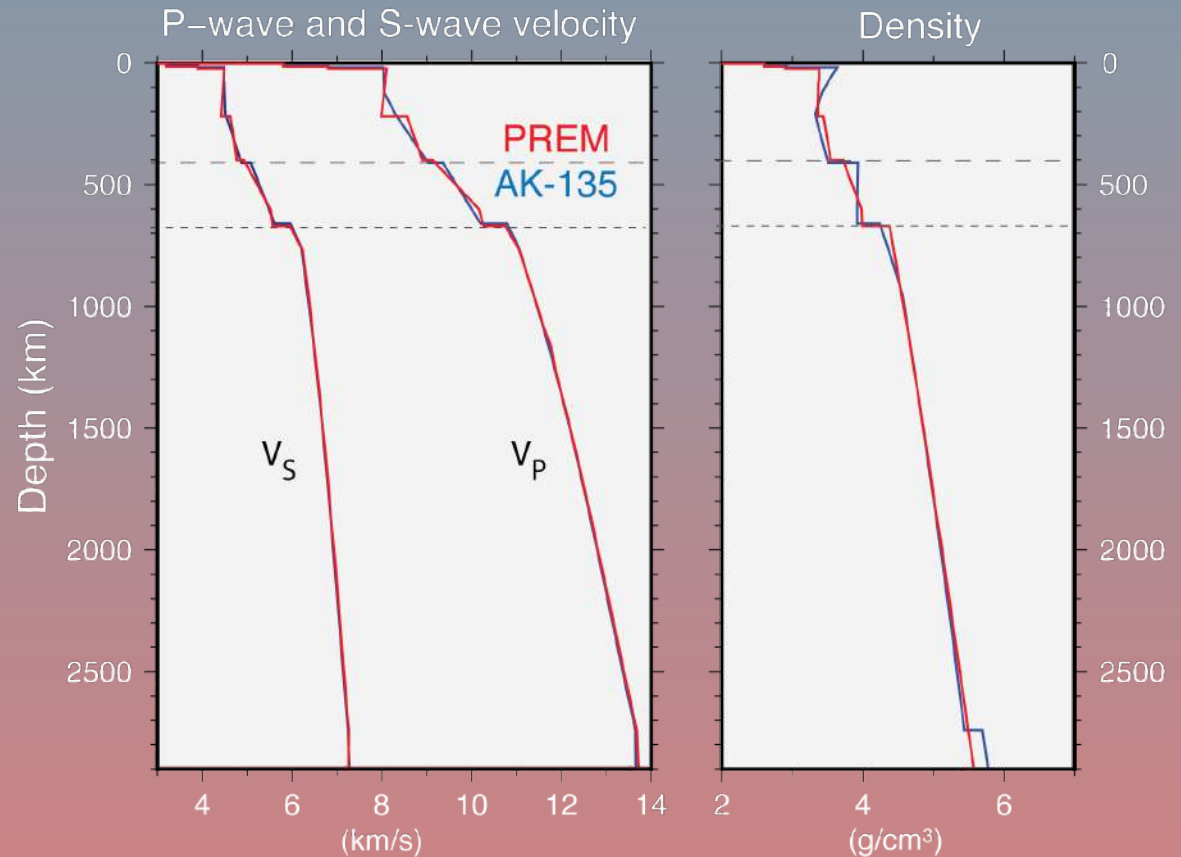
Lower mantle:

- Subducted slabs, mantle plumes, LLSVPs, ULVZs, recycled and primitive features
- Mixing/mass transfer with upper mantle
- Variable modes of convection

Structure of the mantle

Standard 1-D radial density and velocity models

- ‘First order’ phase changes leading to reflections
- Not within the lower mantle

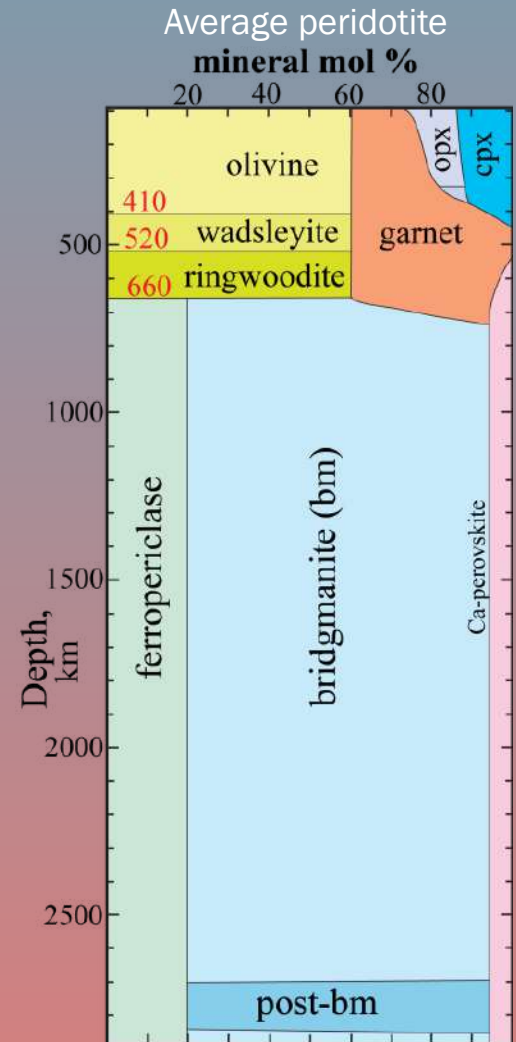


References: Dziewonski et al. (1981); Kennett et al., (1995)

Composition of the mantle

Thought to be a pyrolite and if similar to upper mantle (Mg/Si ratio ~1.27):

- 80% (Mg,Fe)SiO₃ bridgmanite
 - 20% (Mg,Fe)O ferropericlase
 - Minor CaSiO₃ Ca-perovskite (also ppv)
- Mg/Si, Mg/Fe, Ca/Al ratios an outstanding question, as well as Fe partitioning



Composition of the mantle

Bridgmanitic – Pyrolitic – Harzburgitic

Si rich(er)
Bm rich, Fp poor(er)
Imply distinct UM/LM
Rheologically stronger
 $(\text{Mg}+\text{Fe})/(\text{Si}-\text{Ca}) \sim 1$

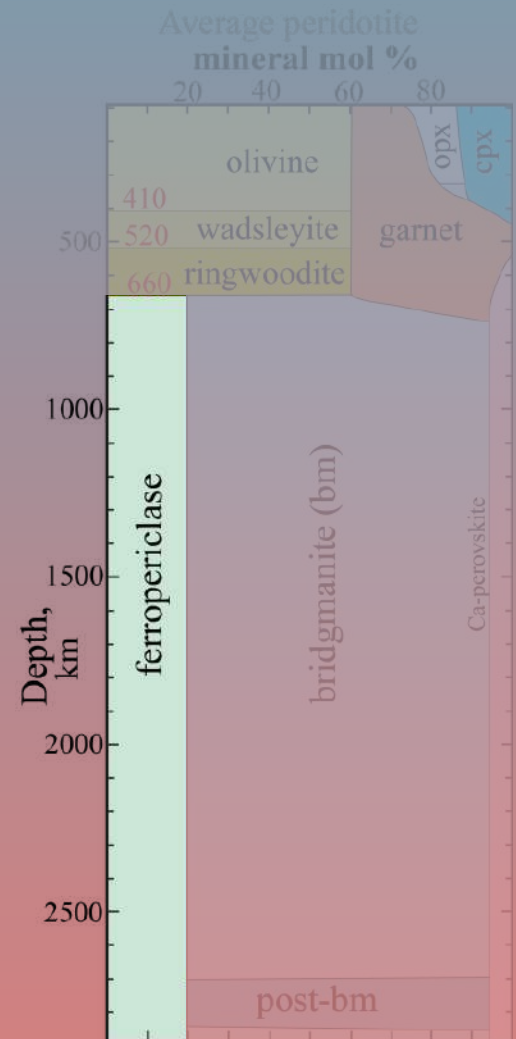
Si poor(er)
Fp rich(er)
Implies mixing
Rheologically variable
 $(\text{Mg}+\text{Fe})/(\text{Si}-\text{Ca}) > 1$

Predicted seismic responses of different compositions greatly affected by temperature therefore not readily discriminated

Composition of the mantle

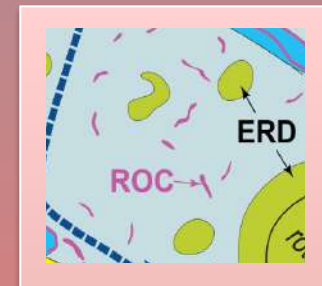
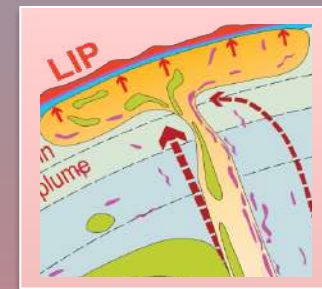
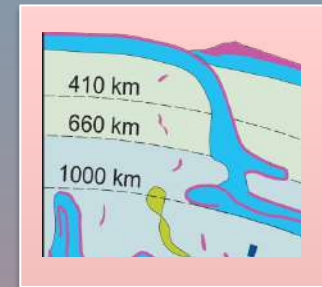
Ferropericlase (Mg,Fe)O

- A major host for iron in the lower mantle
- Fp requires $(\text{Mg}+\text{Fe})/(\text{Si}-\text{Ca}) > 1$
i.e. olivine in addition to pyroxene
- Ferrous iron (Fe^{2+}) cation undergoes electronic transition which affects elastic properties and therefore seismic response
 - Opportunity to constrain composition



So where to look for Fp?

- Slabs...
Fp-rich: 7% basalt and 93% depleted harzburgite
Si-depleted, ~23% Fp
- Plumes...
recycled component, might also contain other Si-rich entrained components
- Ambient...
possibly the least Fp



Things to disentangle (keep in mind)

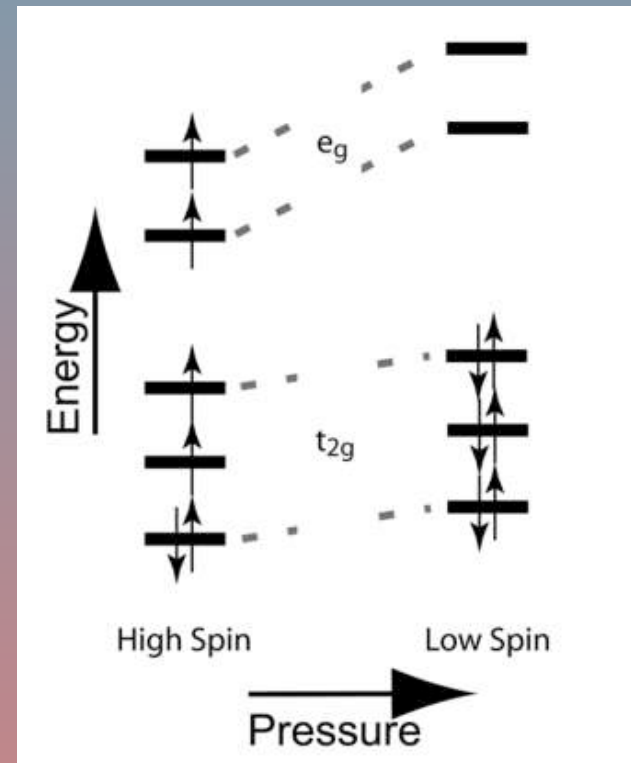
Untangling relatively subtle signals caused by overlapping and/or unconstrained effects:

- Uncertainties in LM material properties, T and composition
- Effects on seismic velocities
- Other mid-mantle changes e.g. viscosity/density change
- Changes in subduction flux
- Influence from pPv and LLSVPs
- Plus others...

Iron Spin Transition

Iron Spin Transition

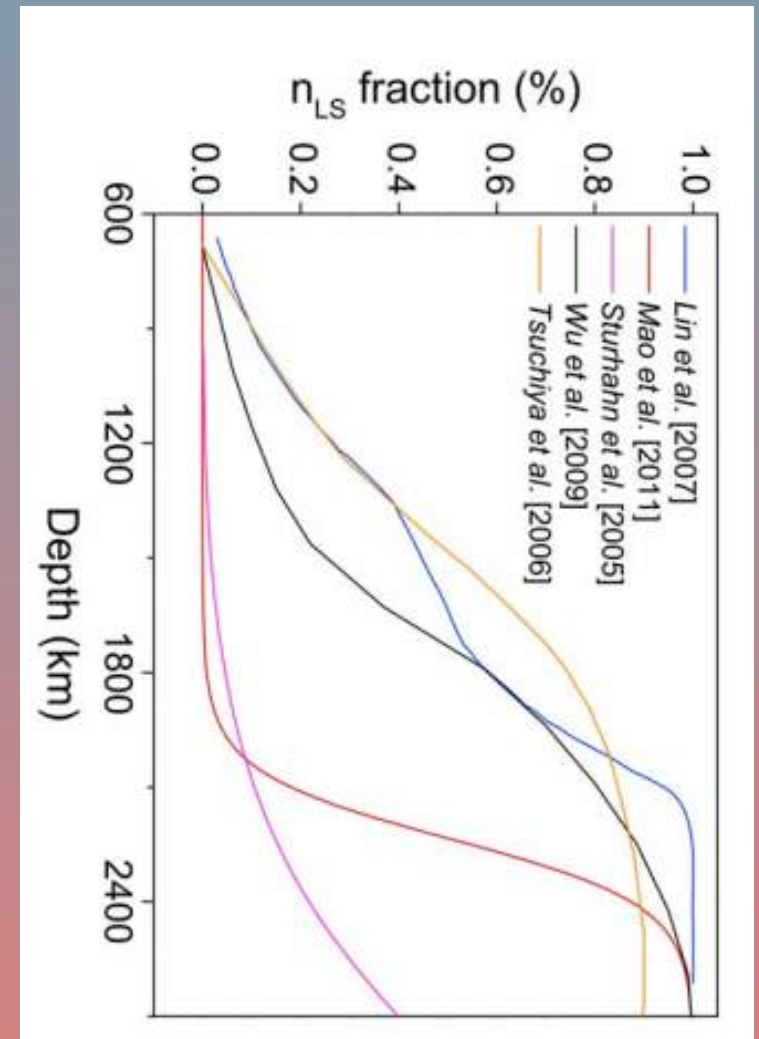
- First proposed by Fyfe (1960)
- Spin transition = pressure induced rearrangement of electrons and energy of chemical bonds (“spin pairing”)
- Collapse of electron orbitals of iron (3d) from high to low spin state
 - Mixed spin/spin transition
- Reduces cation size (volume) changing physical properties of Fp



Speziale et al., 2005

Iron Spin Transition

- Experimentally confirmed by Badro et al. (2003)
 - ~60-70 GPa
 - ~1000-2200 km depth
 - ~1900-2300 K
 - Broad (unlike ordinary phase transitions)
- P-induced but also affected by mantle T and composition, and Fe composition and abundance



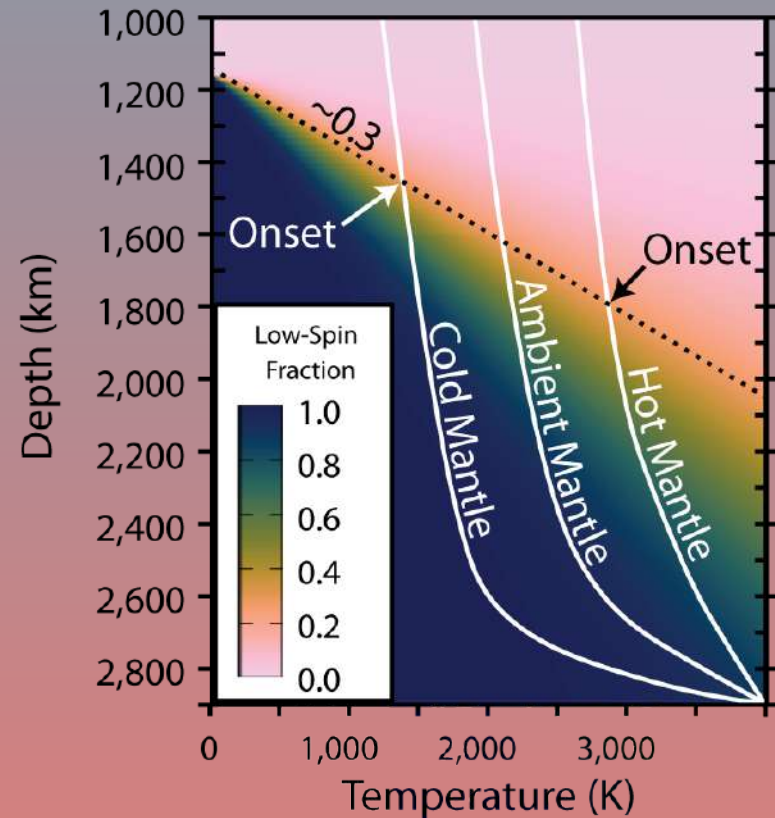
Iron Spin Transition

Fe concentration of $x=18.75\%$ in $\text{FpMg}(1-x)\text{FexO}$

$$n_{\text{LS}} = \frac{1}{1 + \exp(\Delta G(P, T)^* / T)}$$

Promoted by increasing pressure and decreasing temperature:

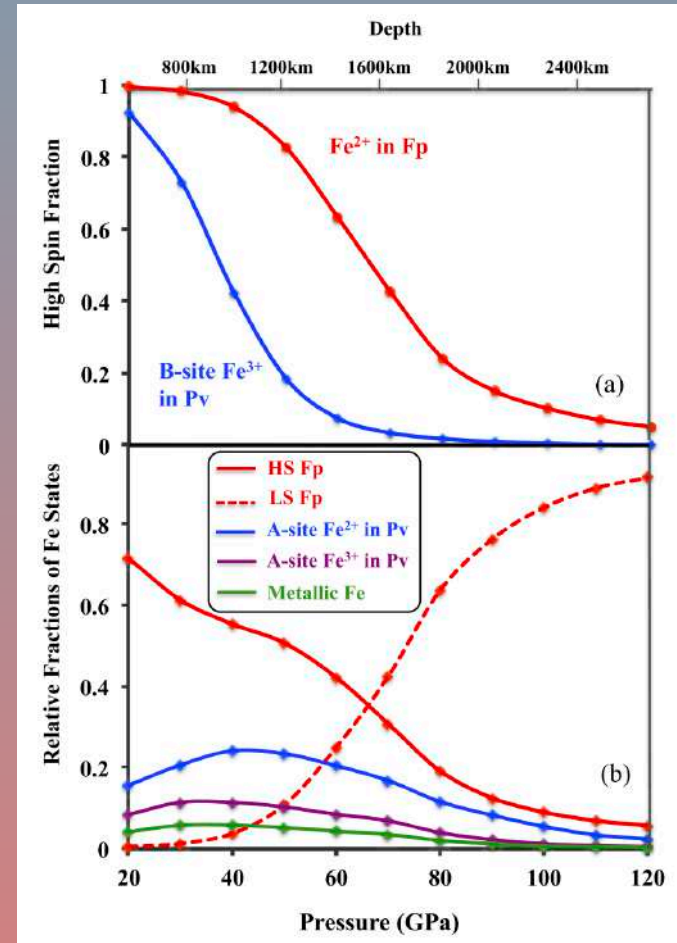
- Increasing width of the mixed phase region
- Cold geotherm: ~1400 km onset
- Hot geotherm: ~1700 km onset.
- Possible presence of mixed spin to CMB



Shephard et al. (in prep)

FAQ: Why not in Bridgmanite?

- Different crystallographic and oxidation states.
- Role of Al ($\text{Fe}^{+2} \rightarrow \text{Fe}^{+3}$)
- Iron is part of Fp backbone, but not for Bm (SiO_6 octahedra are most important structural framework for Bm).



Iron Spin Transition

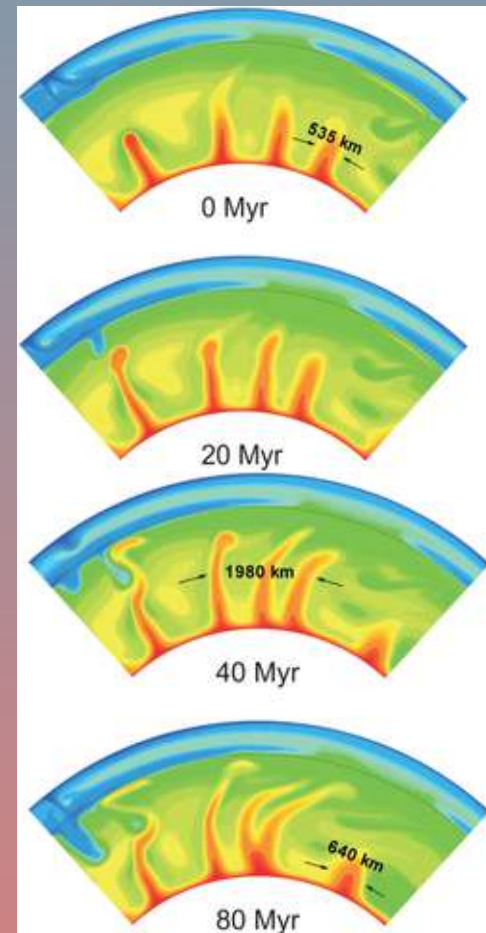
Effects:

Significant effect on density ($\sim 1\%$)

Bulk modulus softens (!)

Little effect on shear modulus

- Changes in viscosity, radiative thermal conductivity, thermal expansion, heat capacity and creep activation parameters, enhancement of anisotropy, convective vigour etc.
- Changes iron partitioning and speciation (suppresses Fe^{3+} and metallic Fe formation)



Shahnas et al. (2016)

(K) Bulk modulus



Hulk Modulus

The ratio of the increase in pressure to resulting fractional change in volume

$$K = -V \frac{dP}{dV}$$

- i.e. the compressibility of the material
- Volume change requires bulk modulus change (!)
- Dramatically softens during the spin cross-over
 - E.g. by ~250 GPa at 300 K for $x = 0.1875$ (Wu et al., 2013)

Spin's seismic expectations

Seismology basics

Mapping of travel time curves to seismic velocities

- P-wave (V_P): Compressional/Dilational
- S-wave (V_S): Shear/Rotational
- Velocities depend on physical properties of the material; elastic moduli and density

$$V_P = \sqrt{\frac{K + \frac{4}{3}\mu}{\rho}} \quad V_S = \sqrt{\frac{\mu}{\rho}}$$

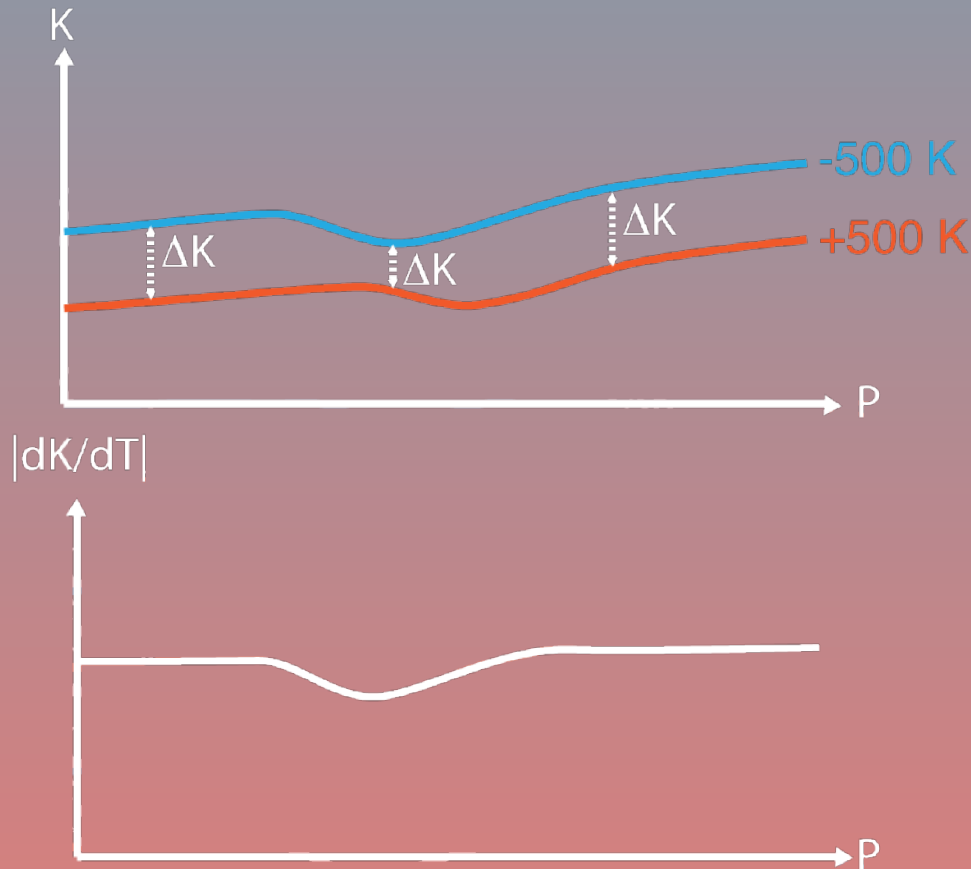
- Affected by temperature, pressure and composition

Spin's seismic predictions

Temperature:

In addition to shifting the pressure range of the spin transition

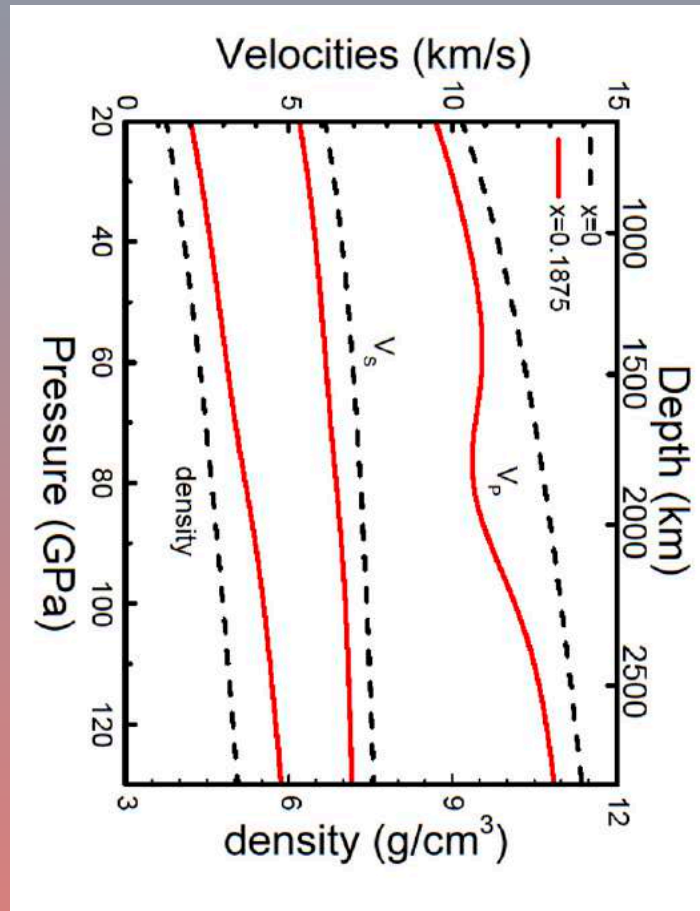
- Reduces sensitivity of V_p to lateral T variations



Spin's seismic predictions

Composition:

- Enhances sensitivity of V_p (and V_ϕ) to composition
 - Increasing Fe/(Fe+Mg) decreases all velocities and enhances effect on V_p



Lin et al. (2013)

Spin's seismic predictions

In short:

- V_p expected to decrease in the transition
- V_s expected to stay the same

AND

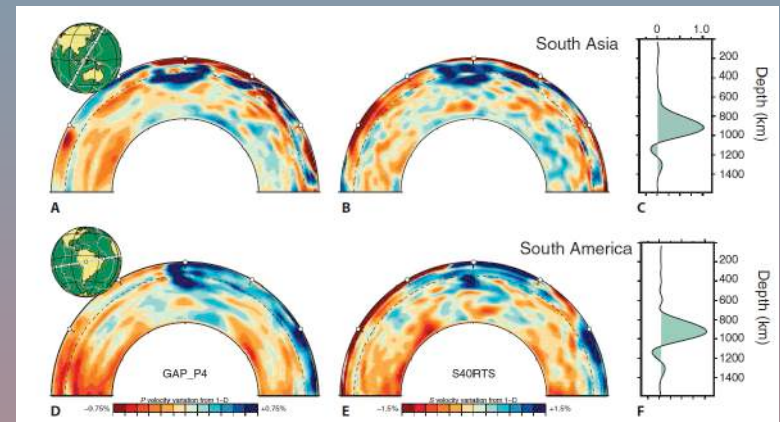
- dV_p/dT decreases in the transition
- dV_s/dT expected to stay the same

**Has it been seismically detected
before?**

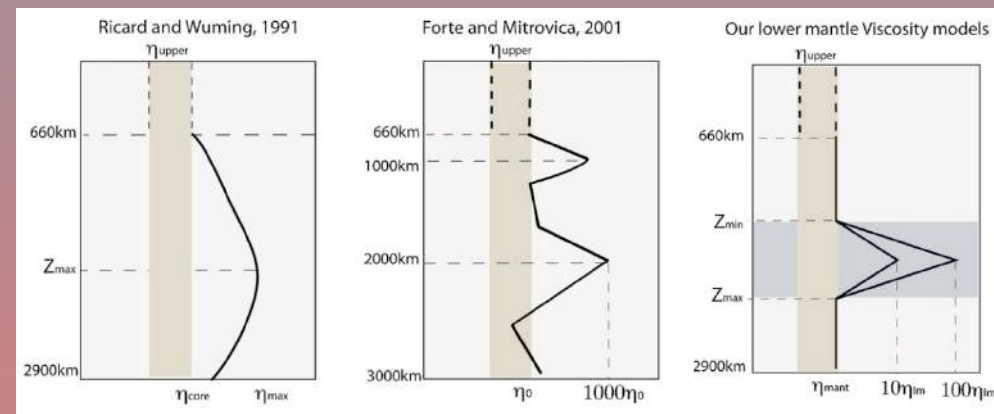
Has it been seismically detected before?

Something's going on:

- Slab stagnation and plume disruption
 - Mid-mantle viscosity/density variation?
 - Dense MORB, Bm-enriched, Bm-dewatering?



Ballmer et al., 2015



Morra et al., 2010

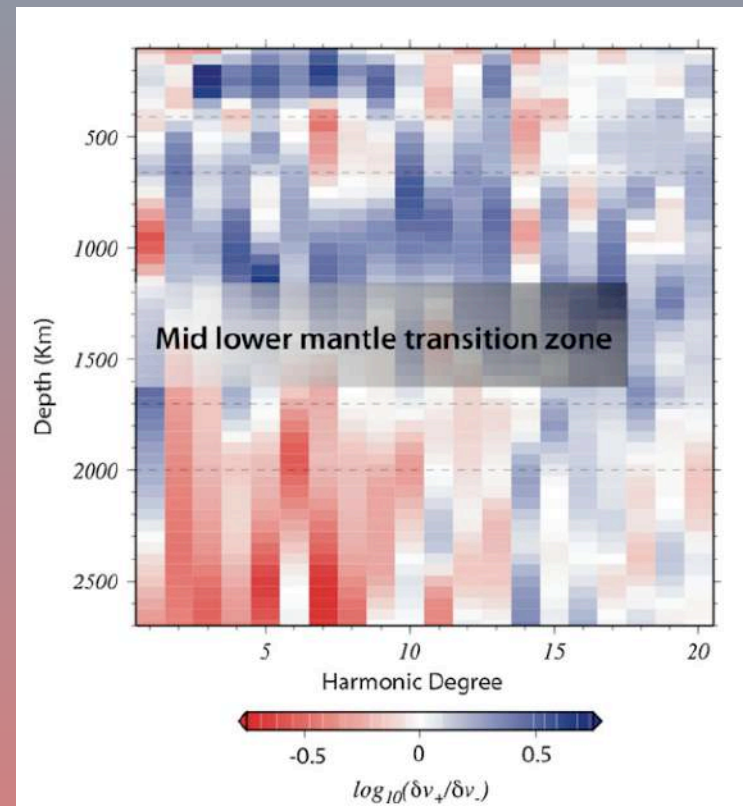
References: Zhao (2007); van der Hilst and Karason (1999); Wu and Wentzkovitch (2014) ; Boschi et al. (2007); Masters (2000) and many others

Has it been seismically detected before?

Something's going on:

- Slab stagnation and plume disruption
 - Mid-mantle viscosity/density variation?
 - Dense MORB, Bm-enriched, Bm-dewatering?
- Spectral changes
 - Anti-correlation of V_S and V_Φ
 - Not necessarily compositional change
 - V_P - V_S ratios

Morra et al., 2010 from Boschi et al., 2010 (SMEAN)

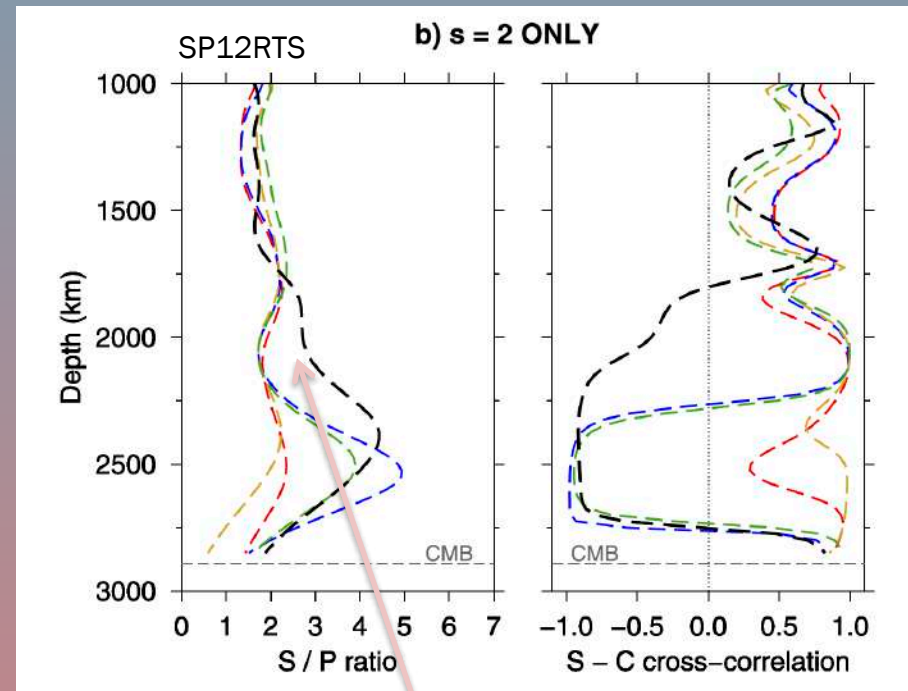


References: Zhao (2007); van der Hilst and Karason (1999); Wu and Wentzkovitch (2014) ; Boschi et al. (2007); Masters (2000) and many others

Has it been seismically detected before?

Something's going on:

- Slab stagnation and plume disruption
 - Mid-mantle viscosity/density variation?
 - Dense MORB, Bm-enriched, Bm-dewatering?
- Spectral changes
 - Anti-correlation of V_S and V_Φ
 - Not necessarily compositional change
 - V_P - V_S ratios



Koelemeijer et al. (2018)

References: Zhao (2007); van der Hilst and Karason (1999); Wu and Wentzkovitch (2014); Boschi et al. (2007); Masters (2000) and many others

**Has it been seismically detected
before?**

The upshot: hinted at but not clearly shown...

FAQ: So what are we doing differently?

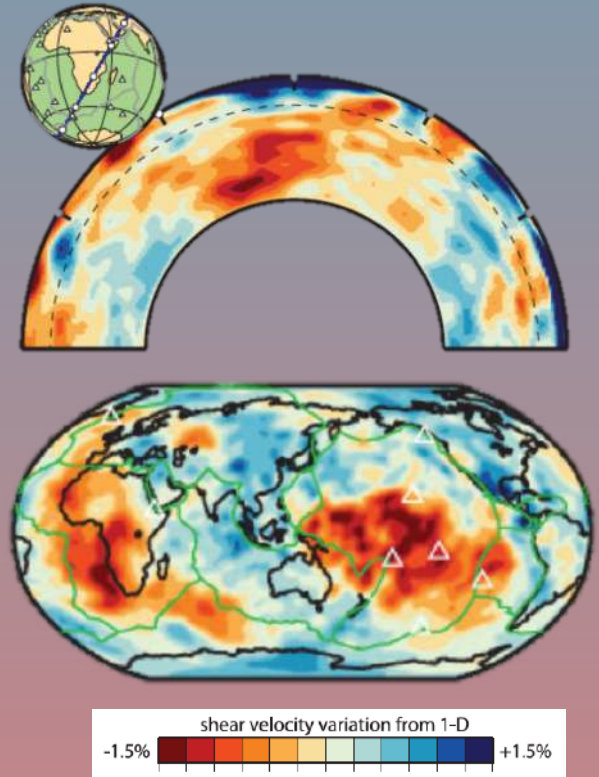
Here we look into

- V_p and V_s
 - fast, slow, and ambient domains
- Multiple tomography models
 - Avoiding those that are similar (e.g. joint inversions)
- Map out the behaviour laterally and radially
 - Quantified in terms of surface area per depth

Seismic tomography

Seismic tomography

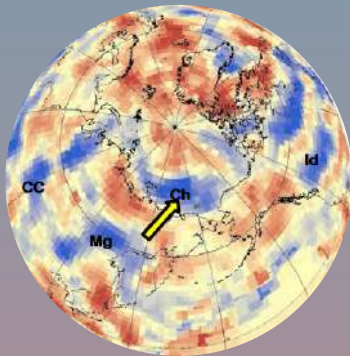
- 3-D velocity structure of the Earth
 - Different seismic phases, methods and approximations
 - Body wave travel times, surface wave dispersion, normal modes
- General agreement on broad structure
 - High velocities = slabs (positive anomalies)
 - Low velocities = plumes, LLSVPs (negative anomalies)
 - V_p and V_s similar resolution in mid-mantle



Ritsema et al. (2011)
S4ORTS

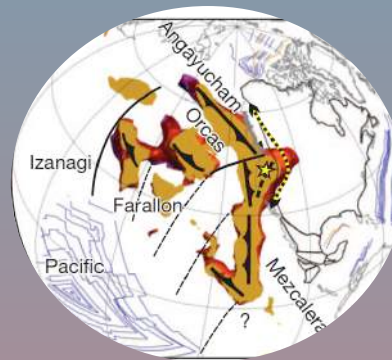
Linking surface and deep

Global, Regional, Absolute frame



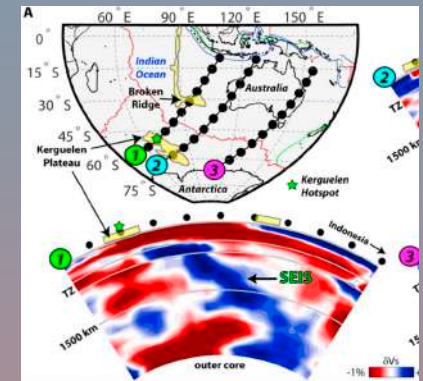
Van der Meer et al. (2010; 2013; 2017)

Regional – Farallon



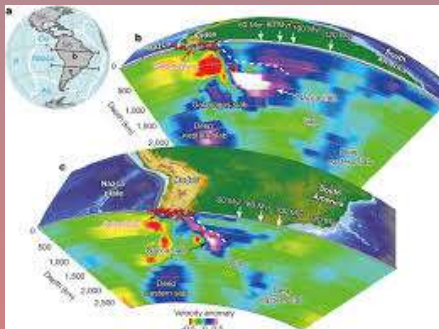
Sigloch and Mihalynuk, 2013

Regional – SE Indian



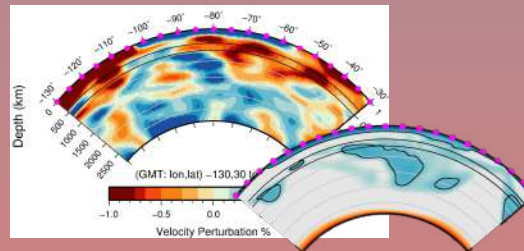
Simmons et al., 2015

Regional – South America

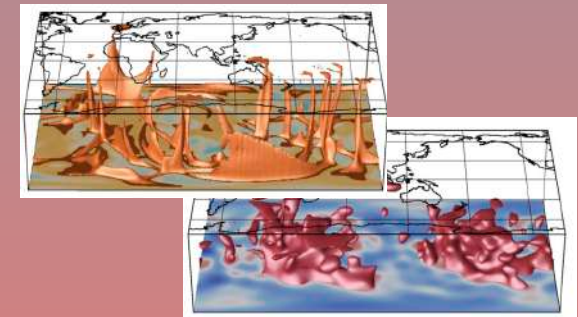


Chen et al., 2019

Numerical modelling



Shephard et al., 2014



Bull et al., 2009

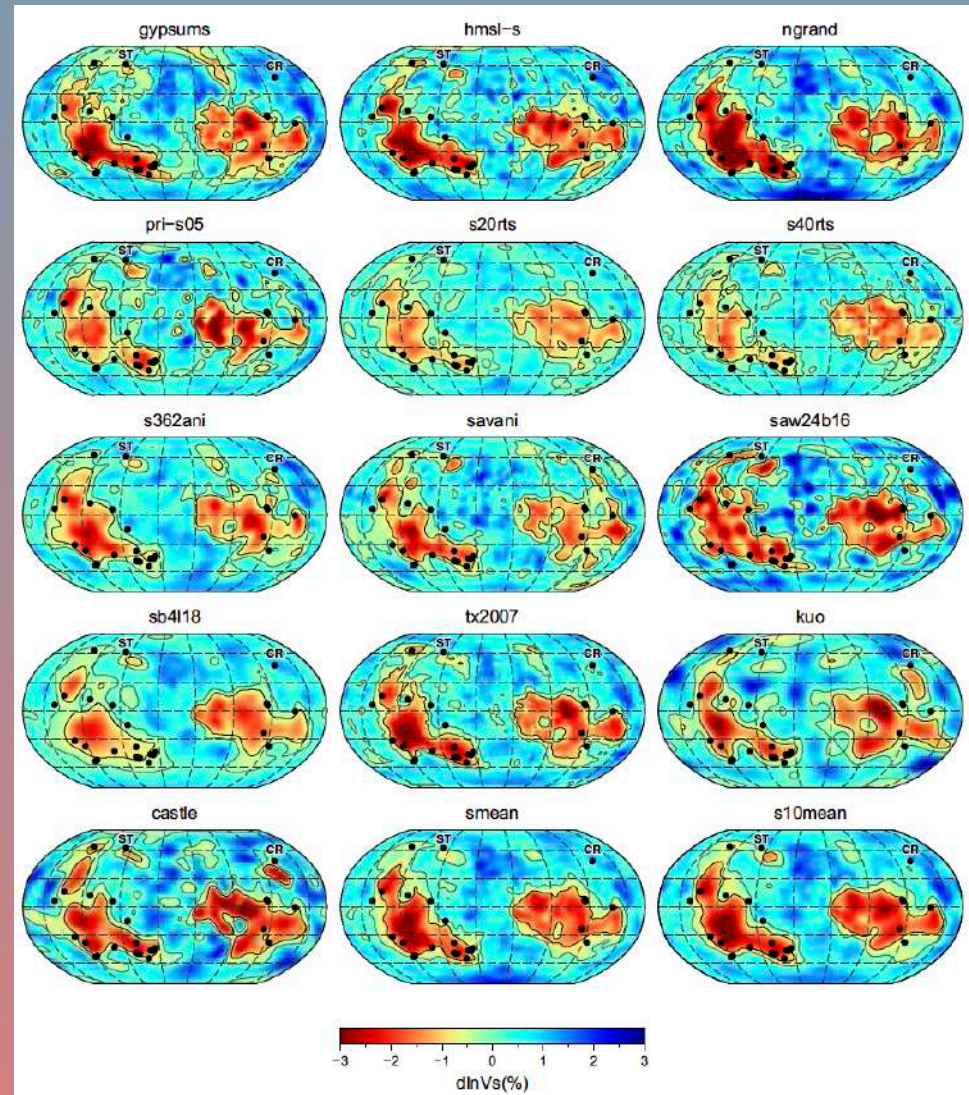
Seismic tomography

Broad spectrum of models to use

Can be difficult to assess resolution and 'reality' of a given model at a given depth/location

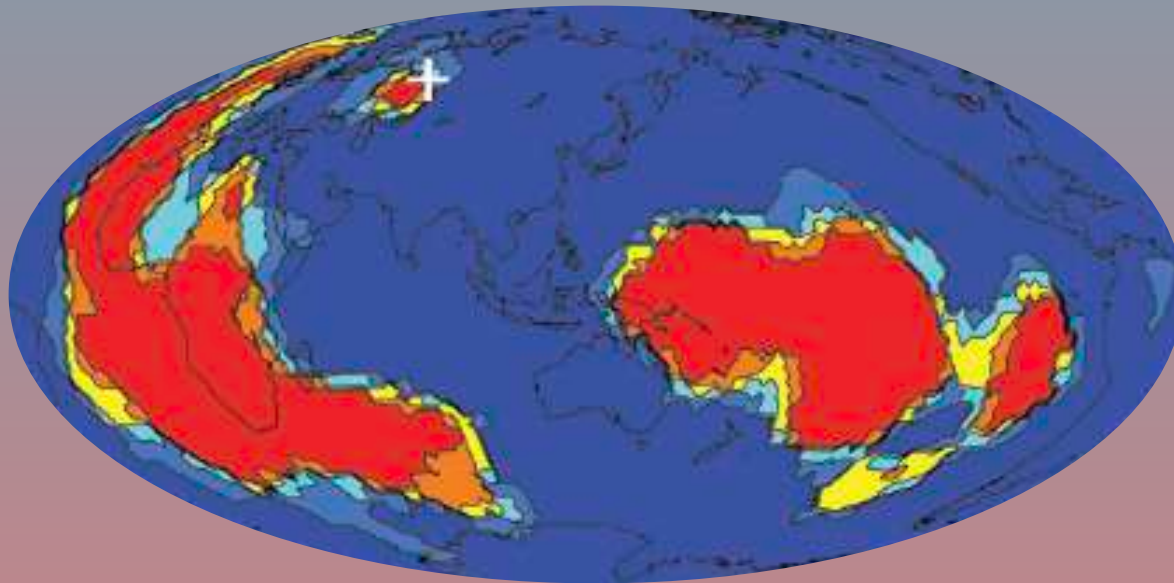
While a V_p/V_s anomaly might result from parameterization choices etc

→ unlikely to persist across numerous models



Seismic tomography

Basically, does a given blue blob really warrant being identified as a slab?



Lekic et al. 2012
Cottaar and Lekic, 2016

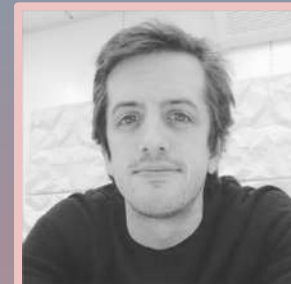
Vote map method



Kara Matthews



Kasra Hosseini



Mathew Domeier

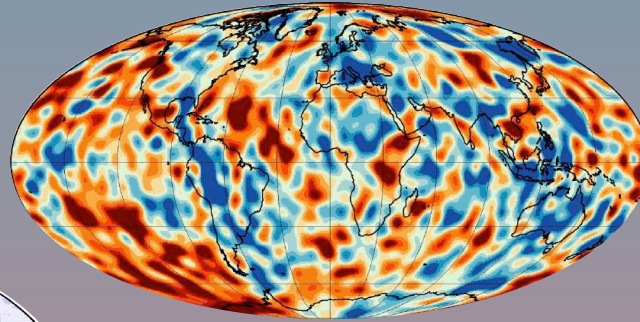
SCIENTIFIC REPORTS

OPEN On the consistency of seismically imaged lower mantle slabs

G. E. Shephard¹, K. J. Matthews², K. Hosseini² & M. Domeier¹

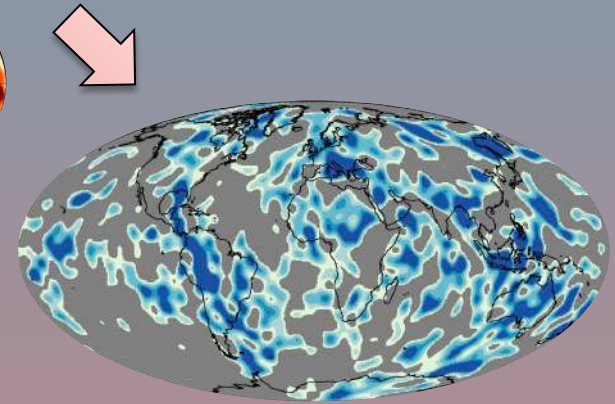
Vote maps

1. Base tomography



% -1 0 1%

*Retain/remove/convert
reference model (mean)*

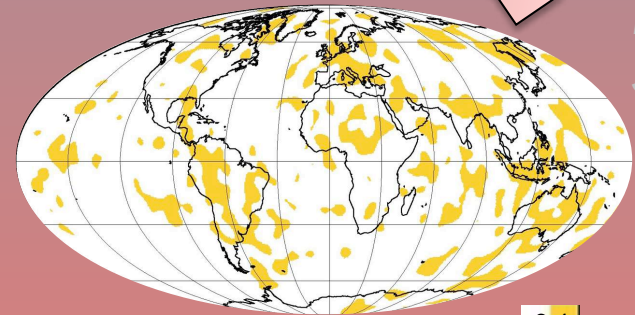


1%

For each depth:

2. Extract positive/negative values

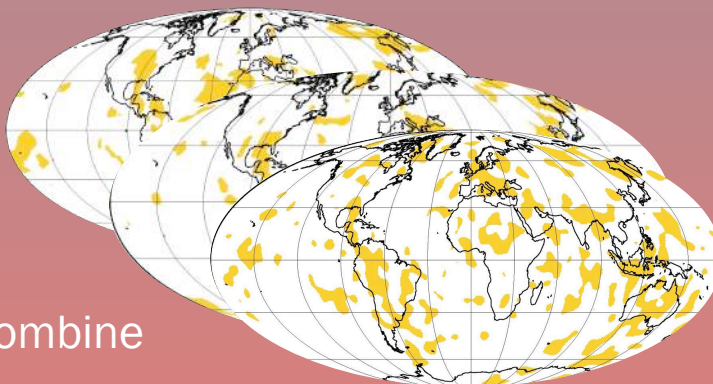
*Mean
RMS
St Dev*



0 1

3. Contour

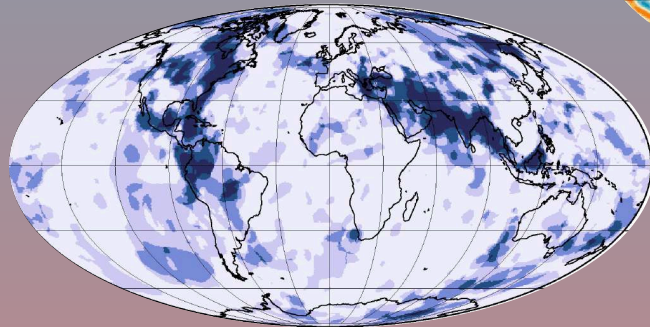
5. Vote map



*P-waves
S-waves*

4. Combine

6. Depth analysis



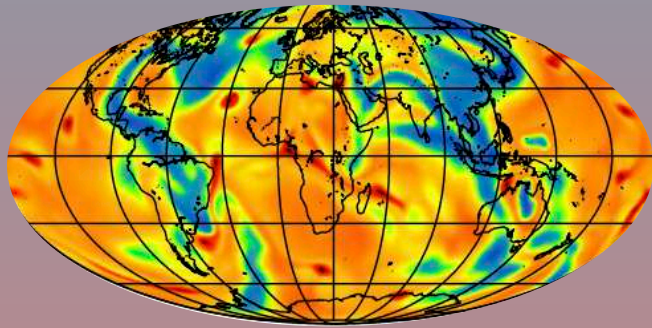
0 4

Applications

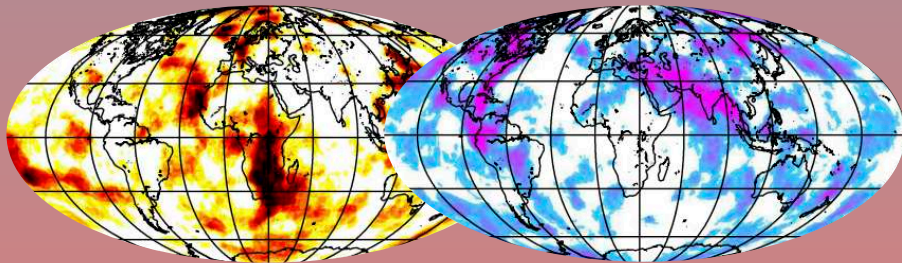
Geodynamics:

Mantle convection modelling

Coltice and Shephard, 2018; JGR



Temp. anomaly



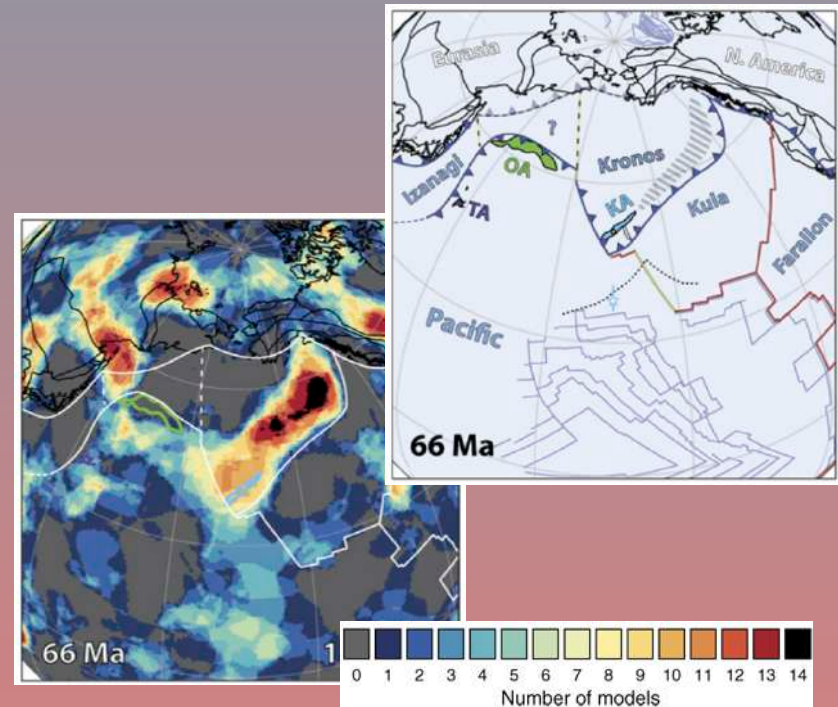
Slow

Fast

Tectonics:

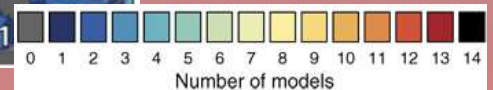
Origin of Hawaiian-Emperor Bend

Domeier et al., 2017; Science Advances

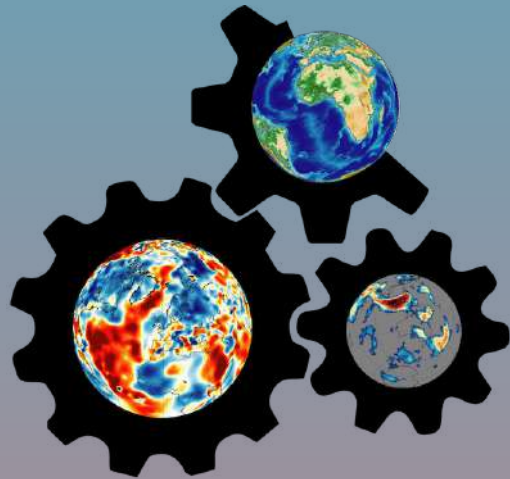


66 Ma

66 Ma



Number of models



SubMachine

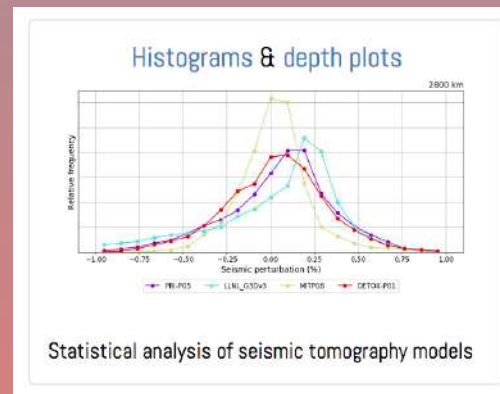
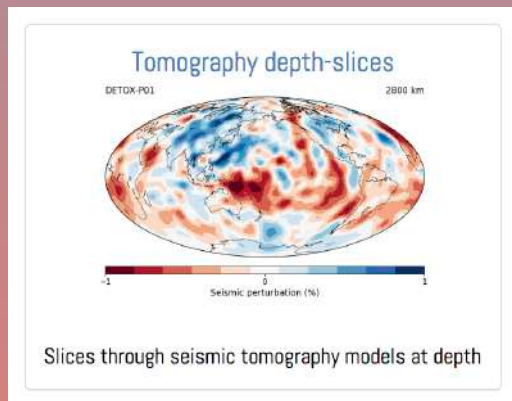
www.earth.ox.ac.uk/~smachine

Web-based tools for the interactive visualisation, analysis, and quantitative comparison of global-scale, volumetric (3-D) data sets of the subsurface

SubMachine

Hosseini et al. (2018)

- Over 30 tomography models →
- BYO Vote maps



P-wave models <input type="checkbox"/>		S-wave models <input type="checkbox"/>	
Global tomography models			
<input type="checkbox"/> GyPSuM-P*	<input type="checkbox"/> GyPSuM-S*	<input type="checkbox"/> GyPSuM-P*	<input type="checkbox"/> GyPSuM-S*
<input type="checkbox"/> HMSL-P06*	<input type="checkbox"/> HMSL-S06*	<input type="checkbox"/> HMSL-P06*	<input type="checkbox"/> HMSL-S06*
<input type="checkbox"/> PRI-P05	<input type="checkbox"/> PRI-S05	<input type="checkbox"/> PRI-P05	<input type="checkbox"/> PRI-S05
<input type="checkbox"/> SP12RTS-P	<input type="checkbox"/> SP12RTS-S	<input type="checkbox"/> SP12RTS-P	<input type="checkbox"/> SP12RTS-S
<input type="checkbox"/> SPani-P*	<input type="checkbox"/> SPani-S*	<input type="checkbox"/> SPani-P*	<input type="checkbox"/> SPani-S*
<input type="checkbox"/> Hosseini2016	<input type="checkbox"/> S20RTS	<input type="checkbox"/> Hosseini2016	<input type="checkbox"/> S20RTS
<input type="checkbox"/> GAP-P4*	<input type="checkbox"/> S362ANI+M*	<input type="checkbox"/> GAP-P4*	<input type="checkbox"/> S362ANI+M*
<input type="checkbox"/> LLNL_G3Dv3*	<input type="checkbox"/> S40RTS	<input type="checkbox"/> LLNL_G3Dv3*	<input type="checkbox"/> S40RTS
<input type="checkbox"/> MITP08*	<input type="checkbox"/> SAVANI*	<input type="checkbox"/> MITP08*	<input type="checkbox"/> SAVANI*
<input type="checkbox"/> MITP_USA_2011MAR*	<input type="checkbox"/> SAW642ANb*	<input type="checkbox"/> MITP_USA_2011MAR*	<input type="checkbox"/> SAW642ANb*
<input type="checkbox"/> MITP_USA_2016MAY*	<input type="checkbox"/> SEMUCB-WM1*	<input type="checkbox"/> MITP_USA_2016MAY*	<input type="checkbox"/> SEMUCB-WM1*
<input type="checkbox"/> UUU-P07*	<input type="checkbox"/> SEMum*	<input type="checkbox"/> UUU-P07*	<input type="checkbox"/> SEMum*
	<input type="checkbox"/> SGL0BE-rani*		<input type="checkbox"/> SGL0BE-rani*
	<input type="checkbox"/> TX2011*		<input type="checkbox"/> TX2011*
	<input type="checkbox"/> TX2015*		<input type="checkbox"/> TX2015*
	<input type="checkbox"/> SEISGLOB1*		<input type="checkbox"/> SEISGLOB1*
	<input type="checkbox"/> SEISGLOB2*		<input type="checkbox"/> SEISGLOB2*
Regional/depth restricted models			
<input type="checkbox"/> Sigloch_Nam_2011	<input type="checkbox"/> 3D2016_09Sv*	<input type="checkbox"/> Sigloch_Nam_2011	<input type="checkbox"/> 3D2016_09Sv*
	<input type="checkbox"/> SL2013sv*		<input type="checkbox"/> SL2013sv*
	<input type="checkbox"/> Zaroli2016		<input type="checkbox"/> Zaroli2016

Vote maps

	P-wave models	S-wave models	
Hosseini et al., 2016/ Hosseini and Sigloch 2015	DETOX-P01	SEMUCB-WM1	French et al., 2014
Obayashi et al., 2013/ Fukao et al., 2013	GAP-P4	SAVANI	Auer et al., 2014
Houser et al., 2008	HMSL-P06	HMSL-S06	Houser et al., 2008
Burdick et al., 2012	MITP_2011	S40RTS	Ritsema et al. 2011

body \pm surface \pm normal modes \pm waveform inversions

0.5° grid spacing

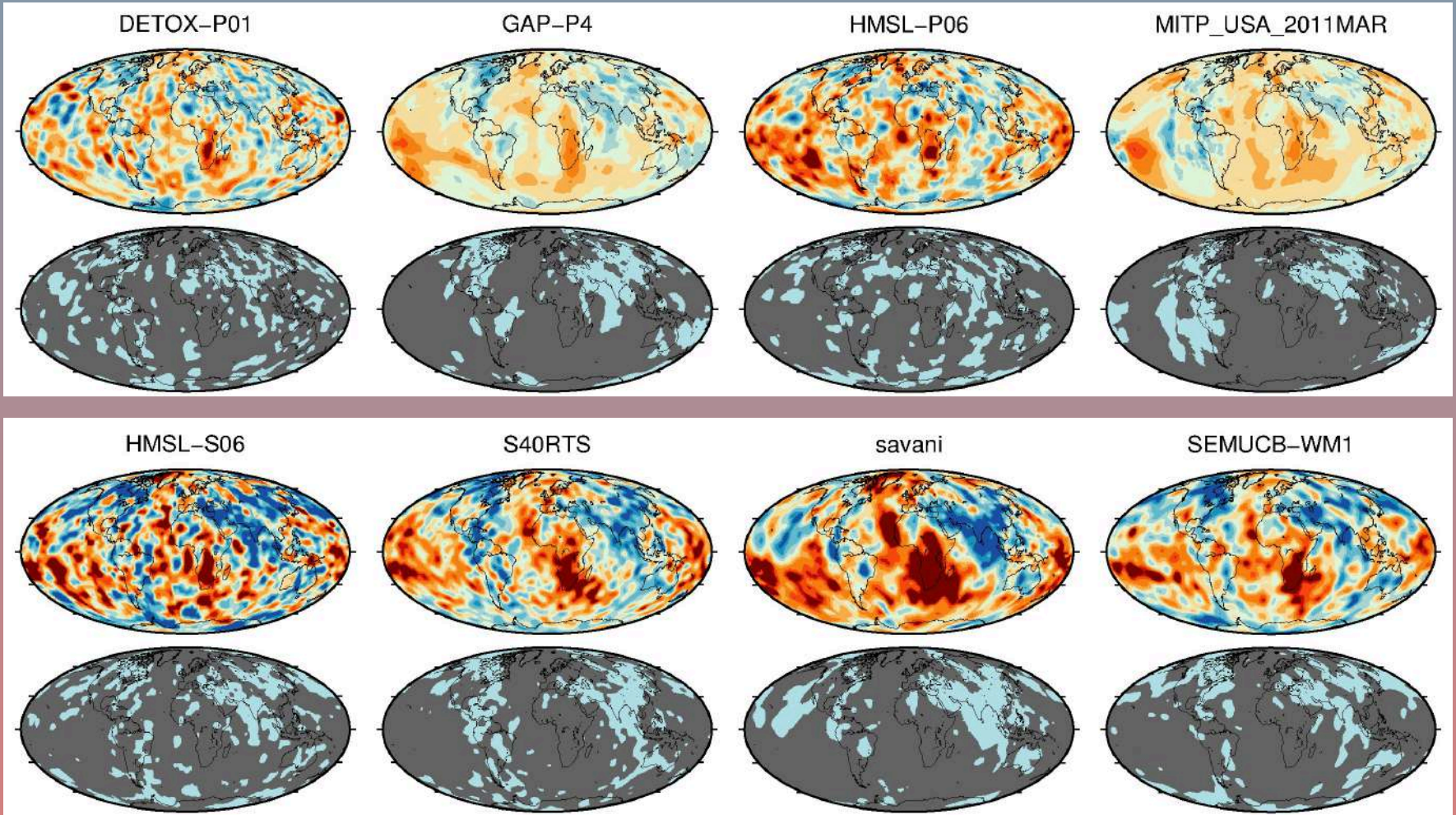
50 km increments

Processed with GMT v5.3.1

Vote maps

Fast anomalies

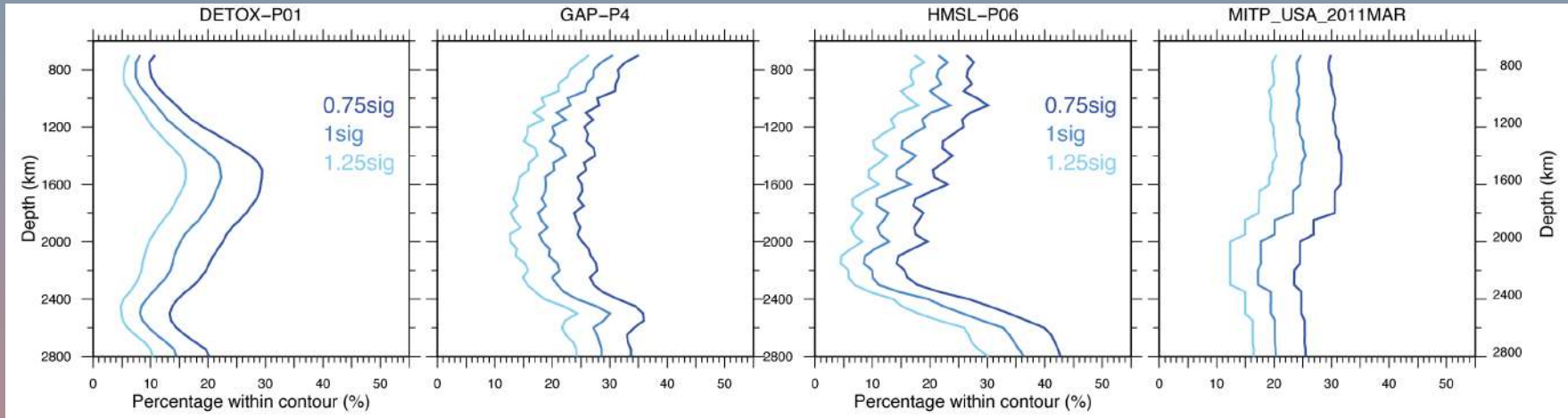
contour $>+1\sigma$ 1800 km



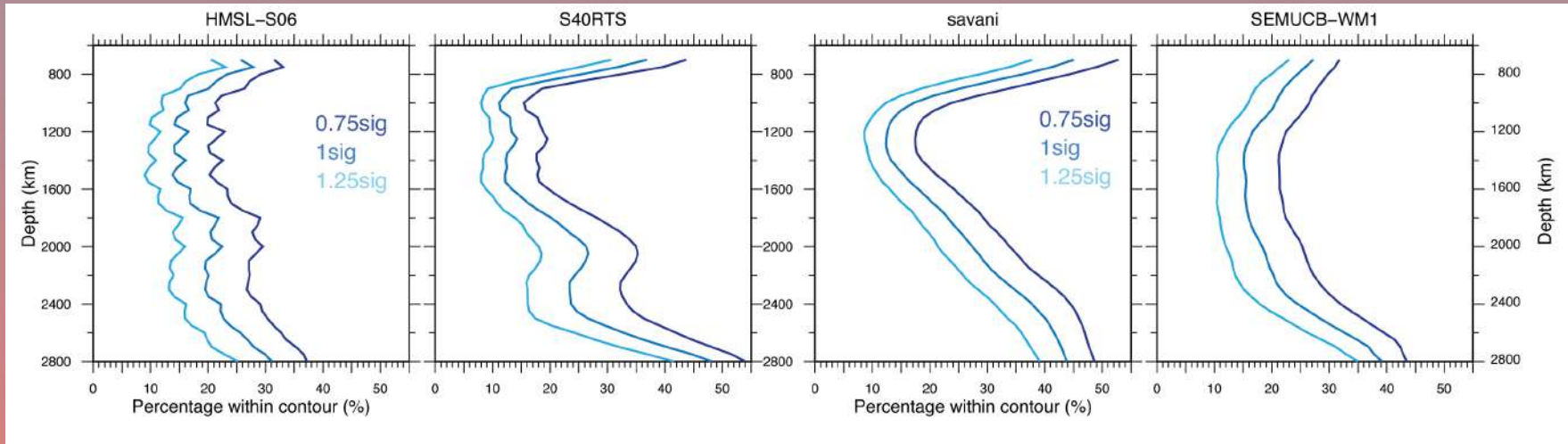
Vote maps – contour

Fast anomalies

P-waves



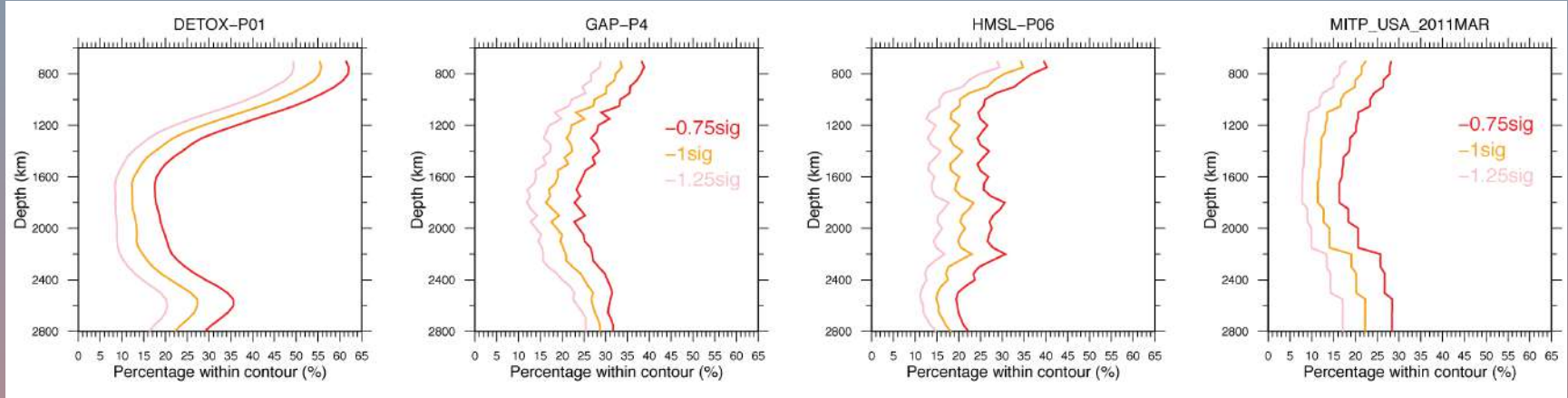
S-waves



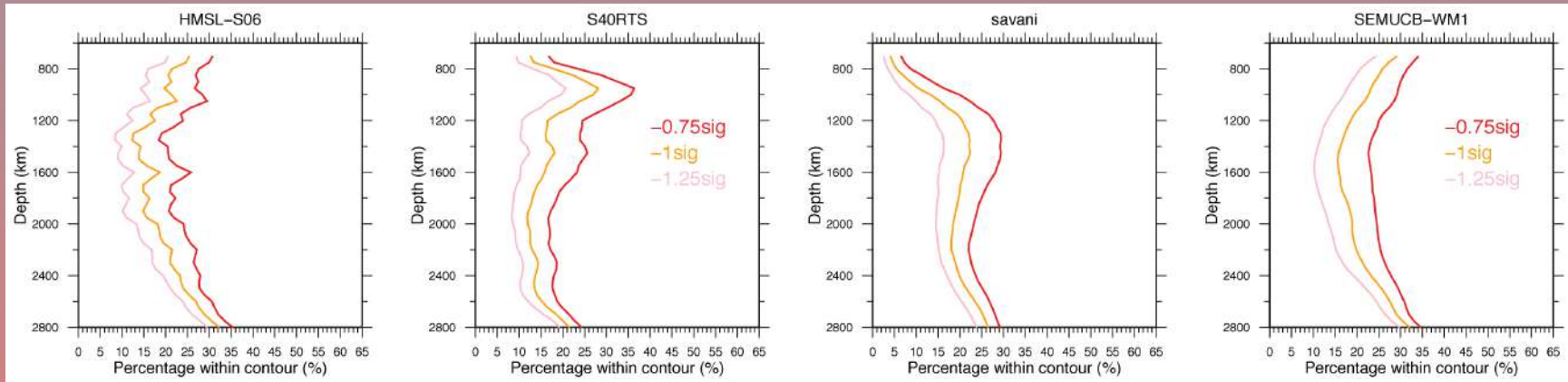
Vote maps – contour

Slow anomalies

P-waves



S-waves

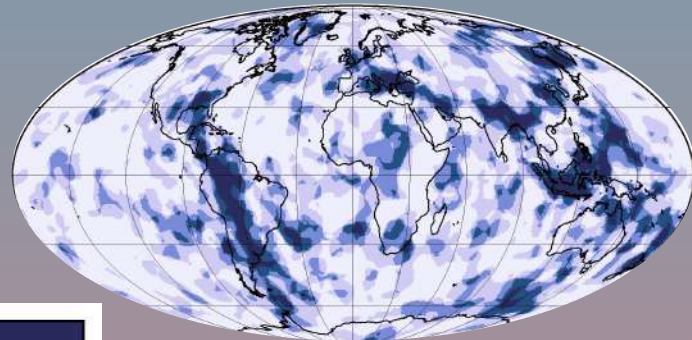
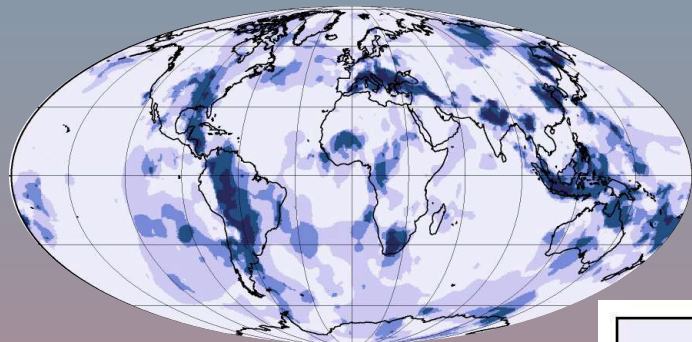


Fast anomalies

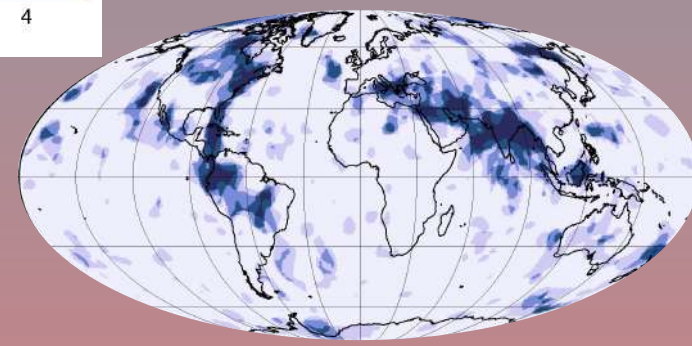
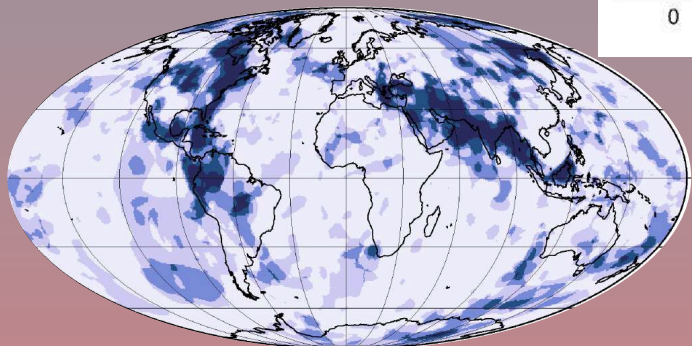
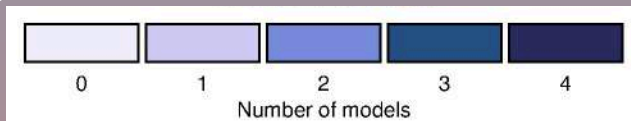
$>+1\sigma$

V_P

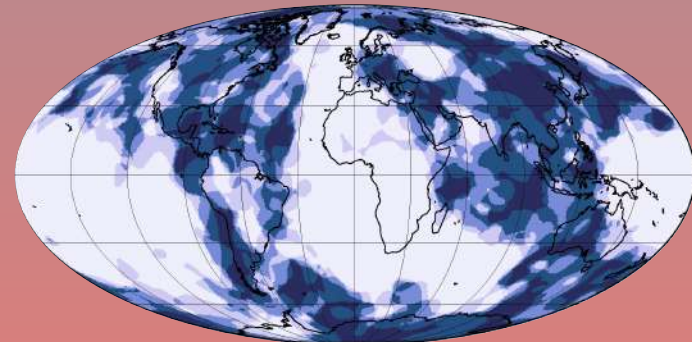
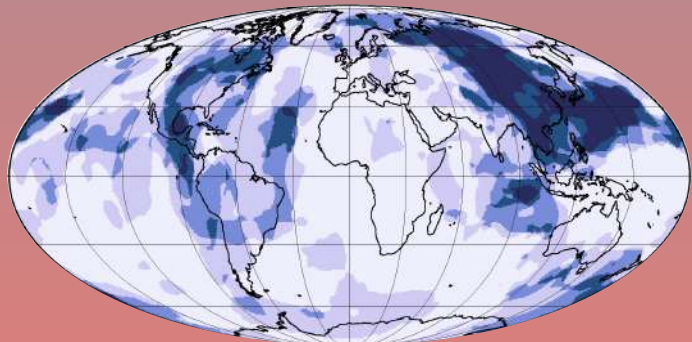
V_S



800 km



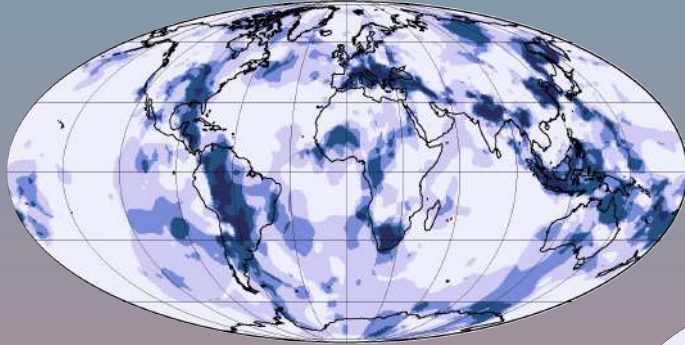
1400 km



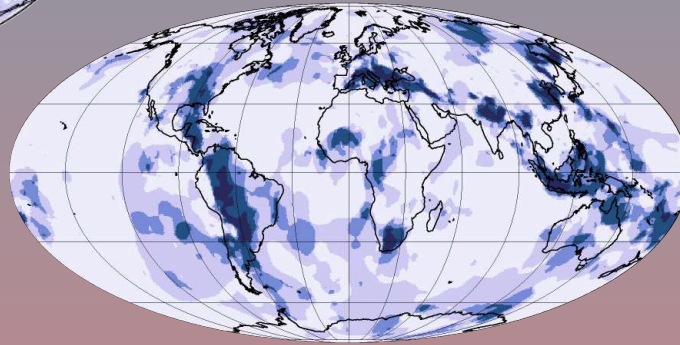
2800 km

Influence of sigma

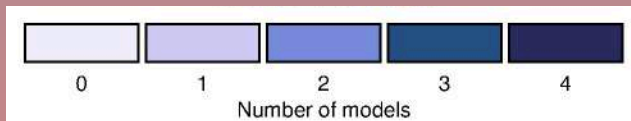
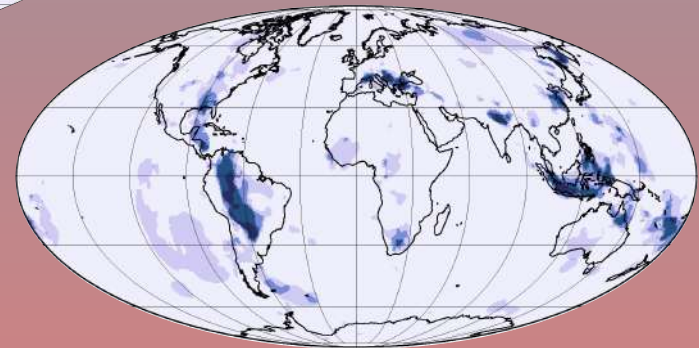
$>+0.75\sigma$



$>+1\sigma$



$>+2\sigma$



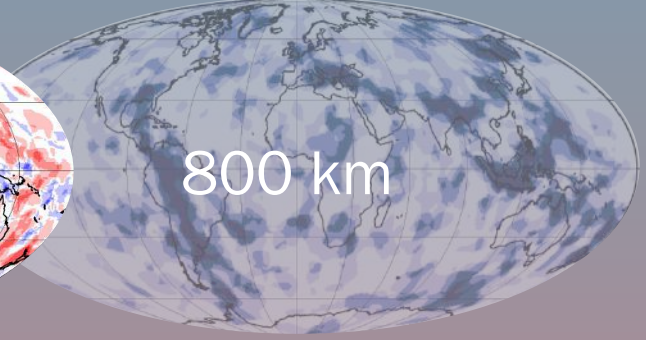
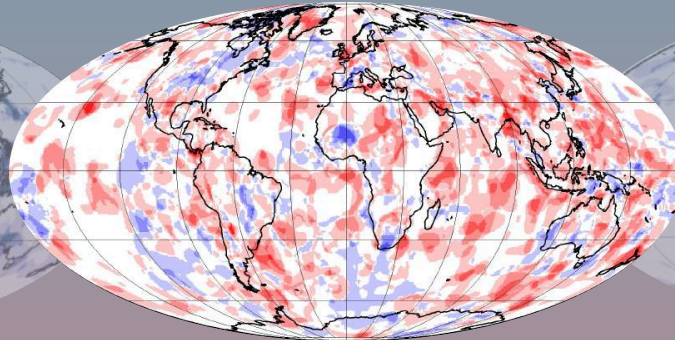
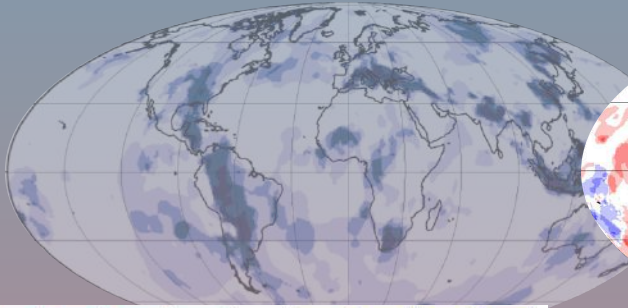
$>+1\sigma$

Fast anomalies

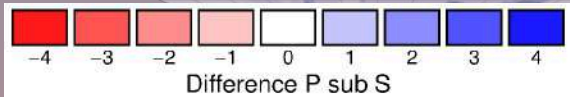
V_P

$V_P - V_S$

V_S

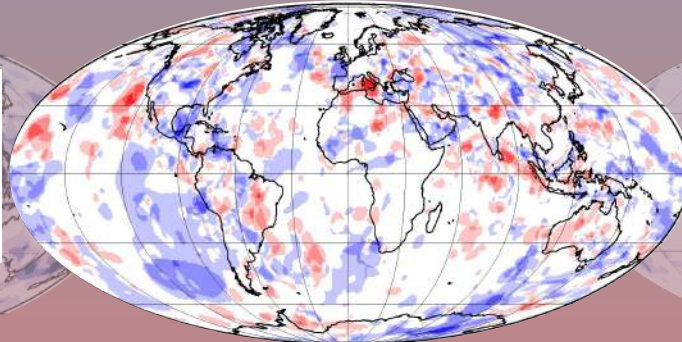


800 km

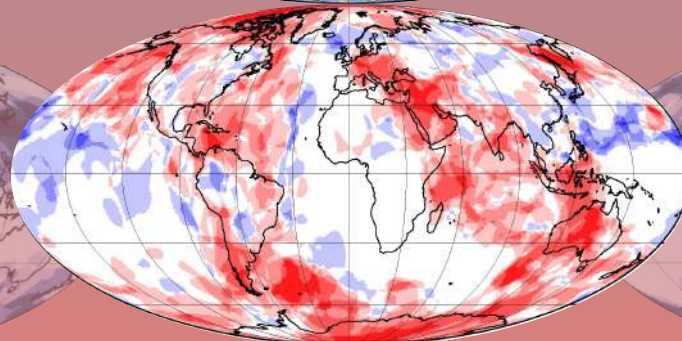
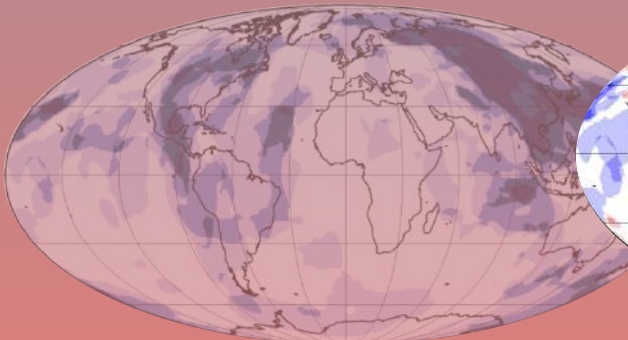


More
S-wave
votes

More
P-wave
votes



1400 km



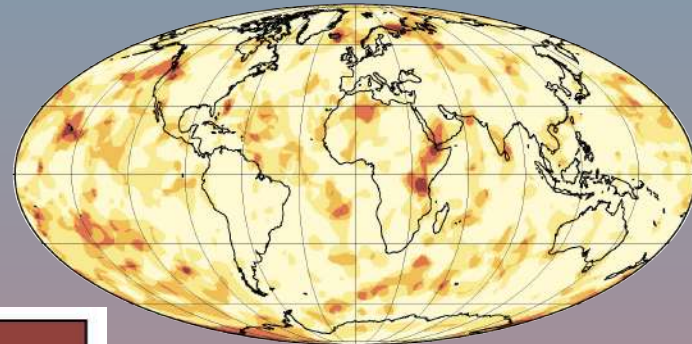
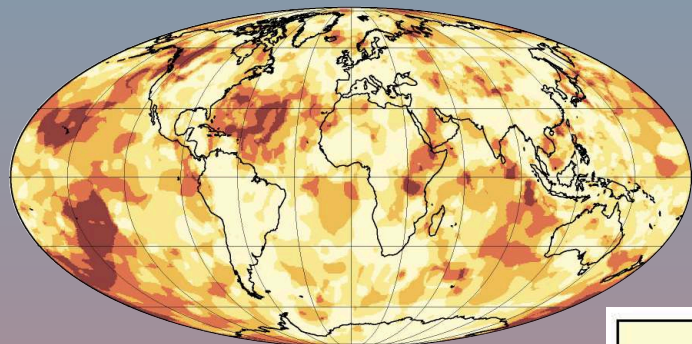
2800 km

Slow anomalies

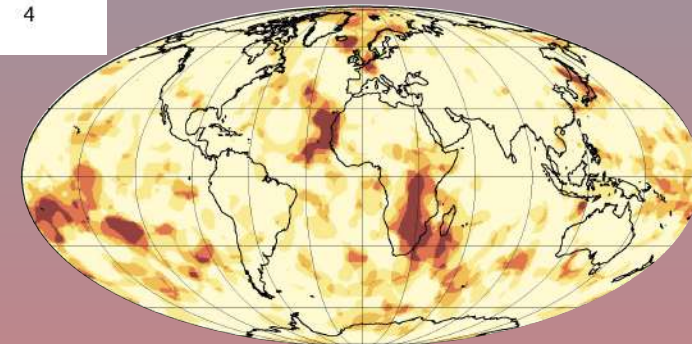
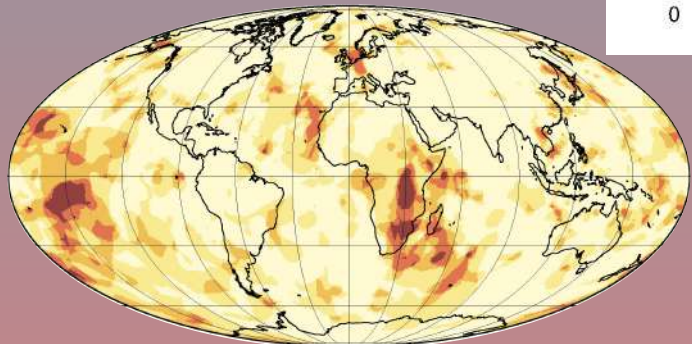
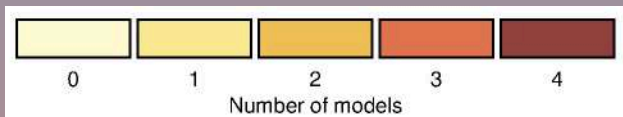
$< -1\sigma$

V_P

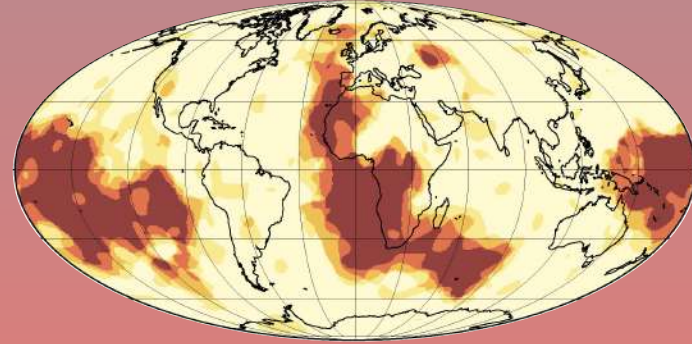
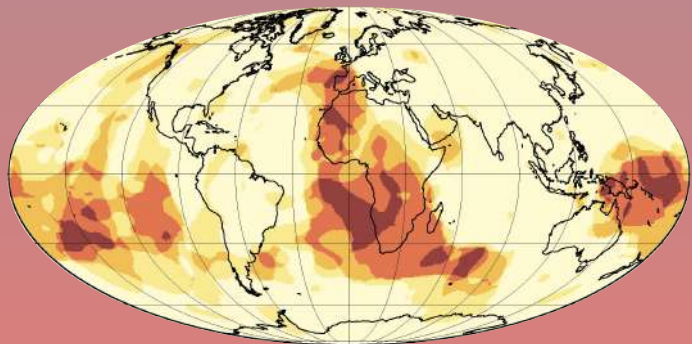
V_S



800 km



1400 km



2800 km

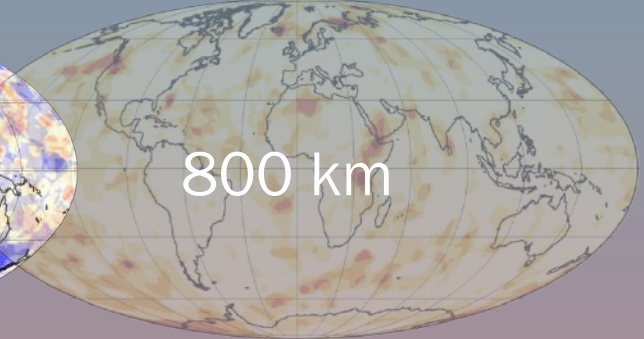
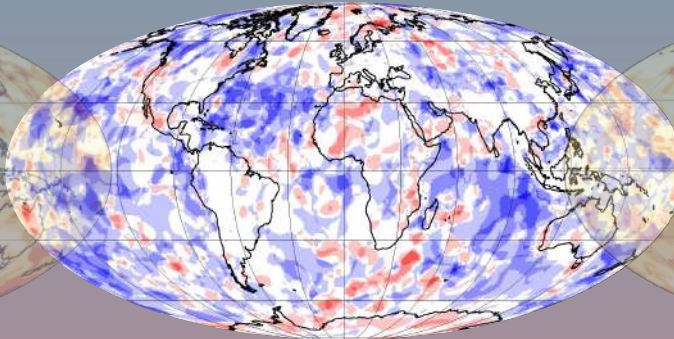
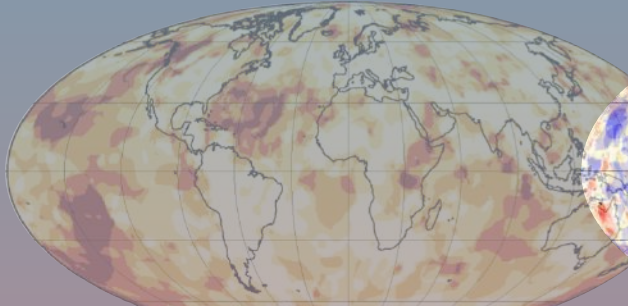
$< -1\sigma$

Slow anomalies

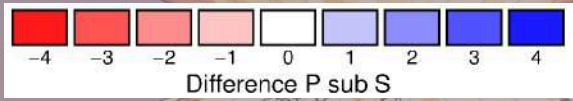
V_P

$V_P - V_S$

V_S

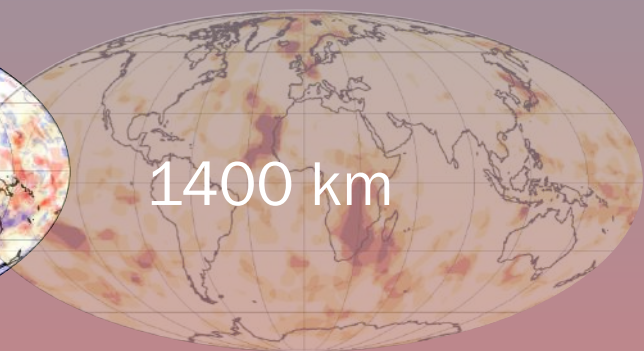
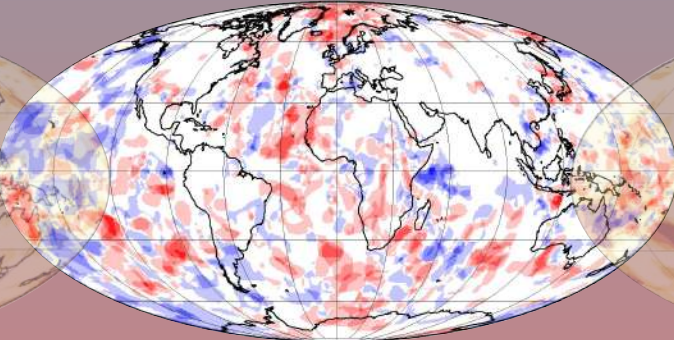
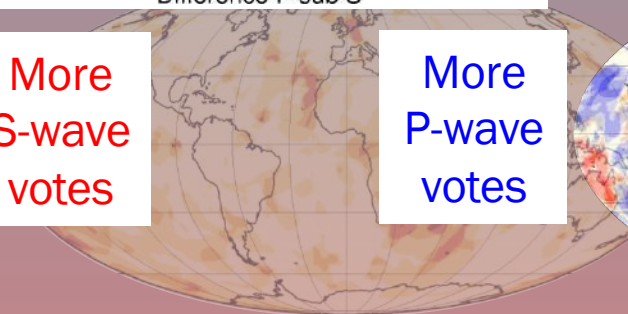


800 km

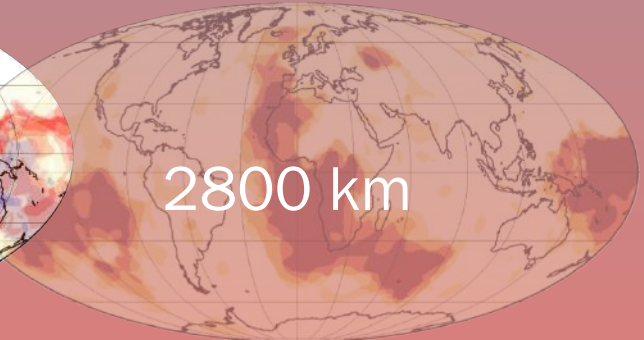
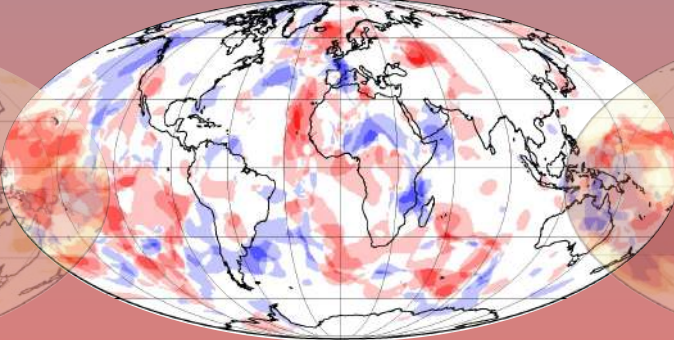
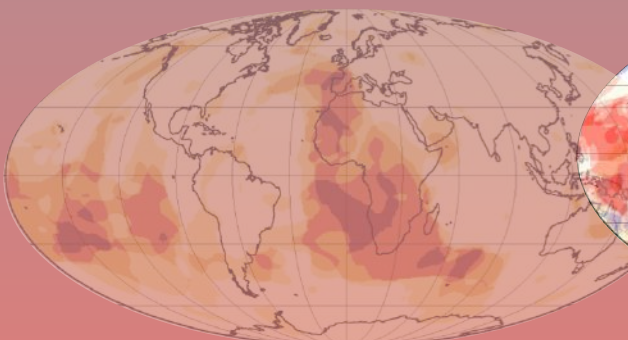


More S-wave votes

More P-wave votes



1400 km



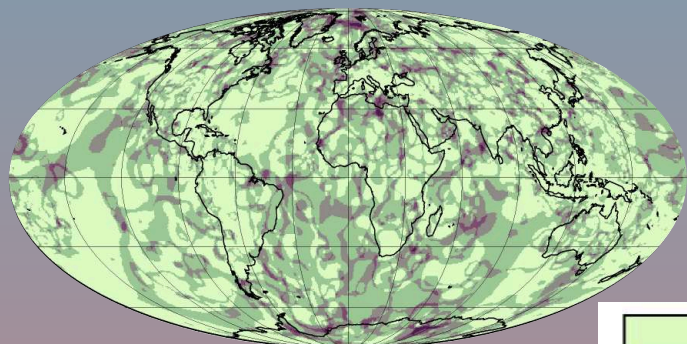
2800 km

Ambient “anomalies”

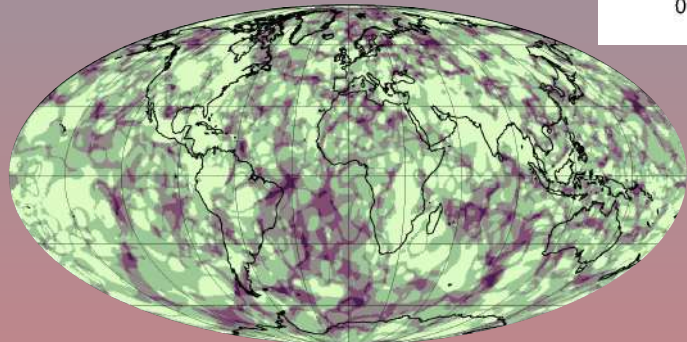
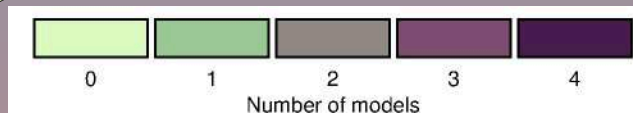
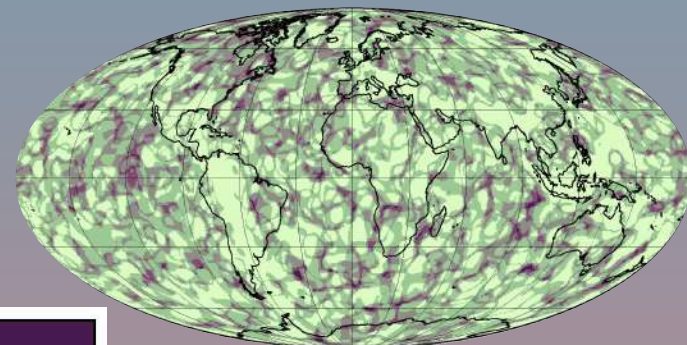
$\pm 0.5\sigma$

V_P

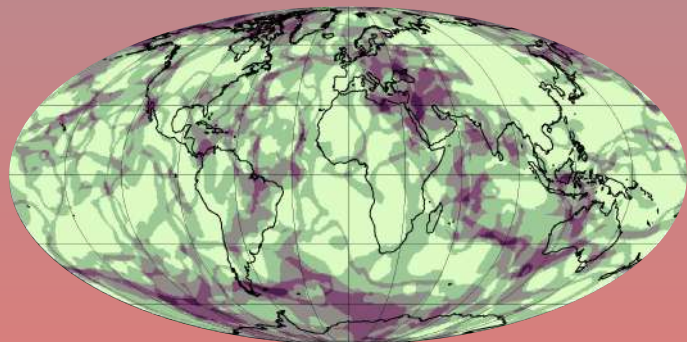
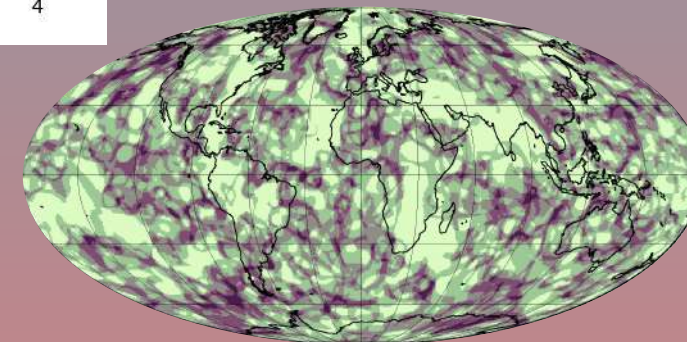
V_S



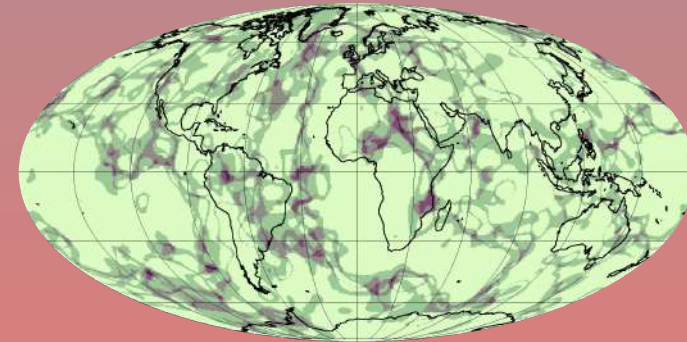
800 km



1400 km



2800 km



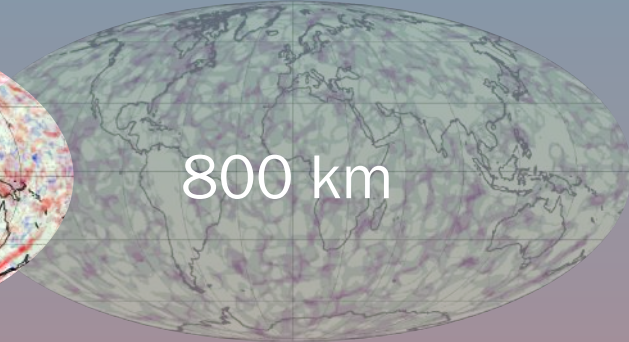
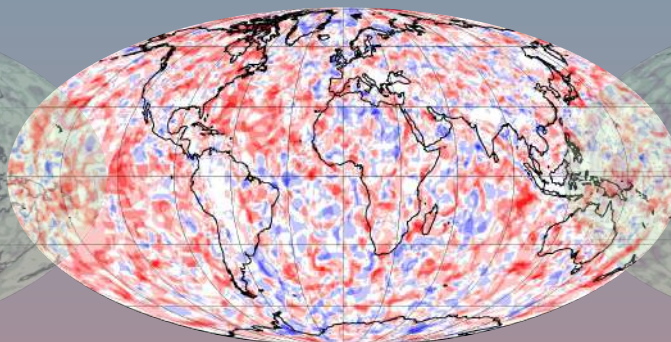
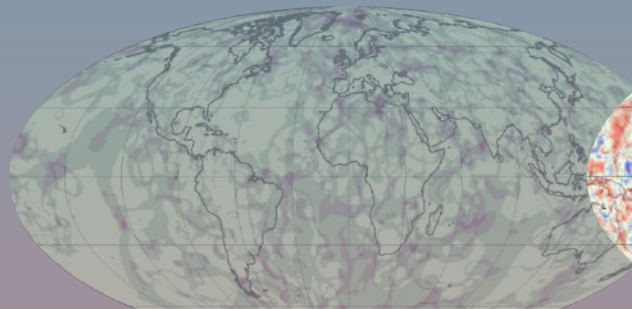
Ambient “anomalies”

$\pm 0.5\sigma$

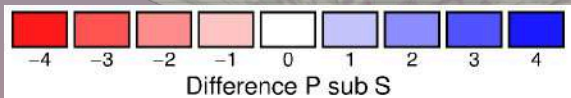
V_P

$V_P - V_S$

V_S

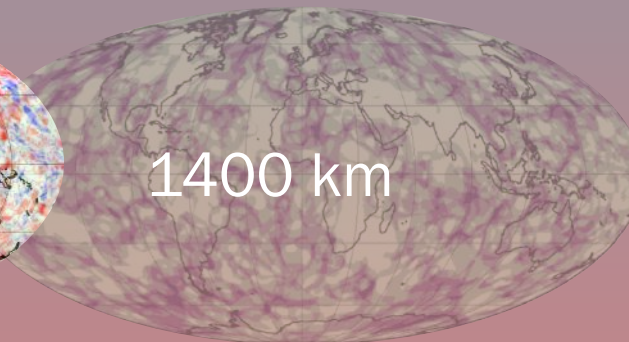
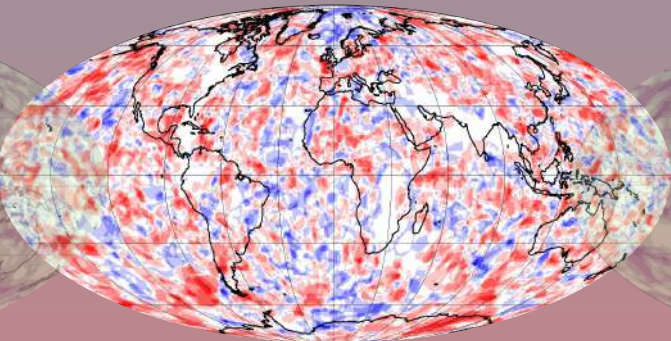
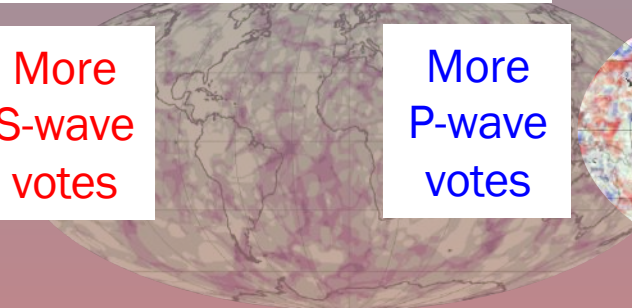


800 km

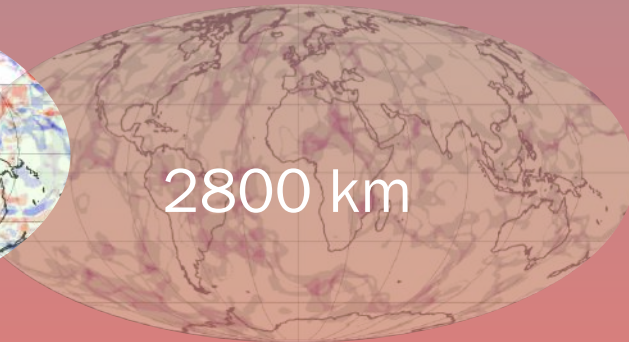
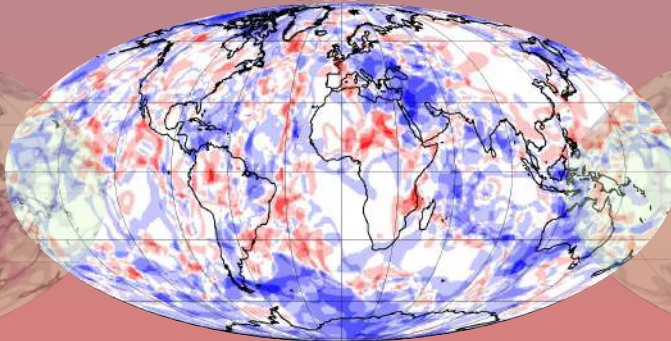
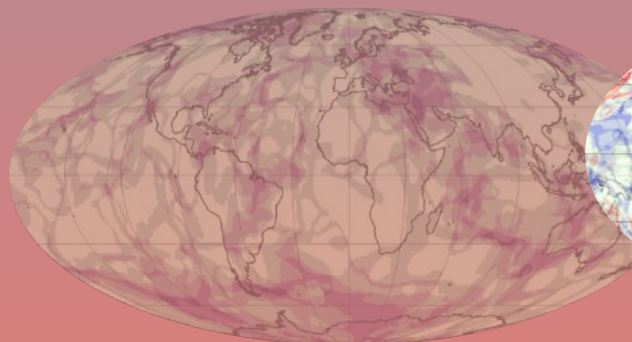


More
S-wave
votes

More
P-wave
votes

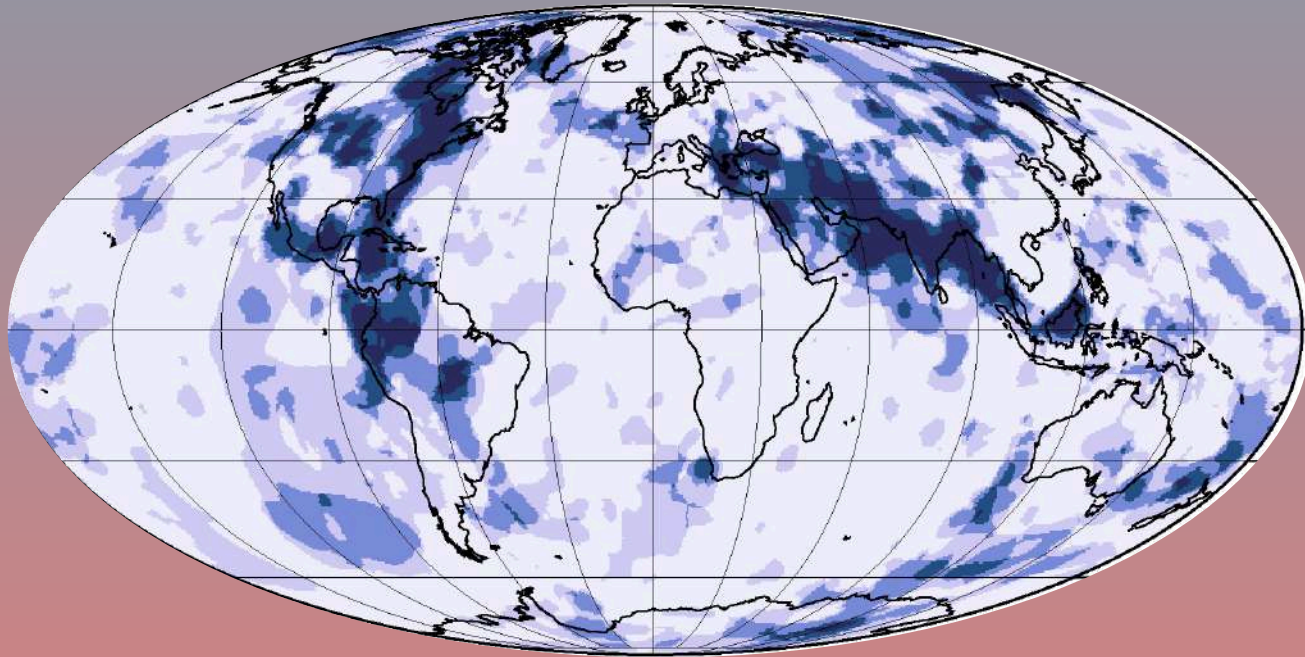
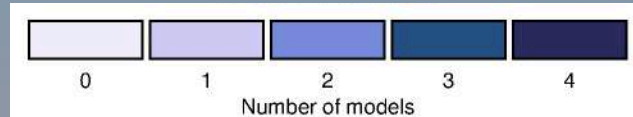


1400 km



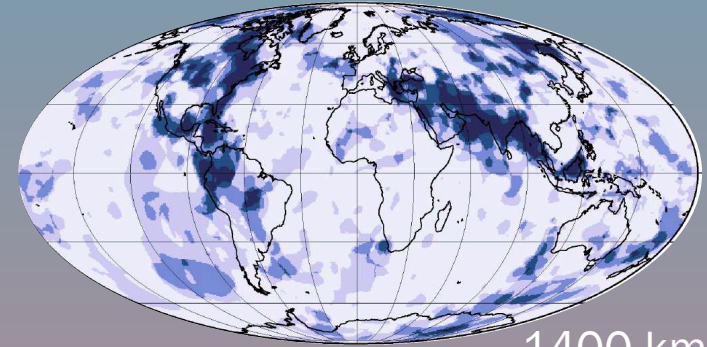
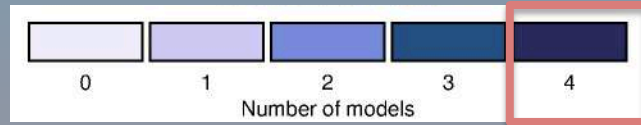
2800 km

Surface area calculations

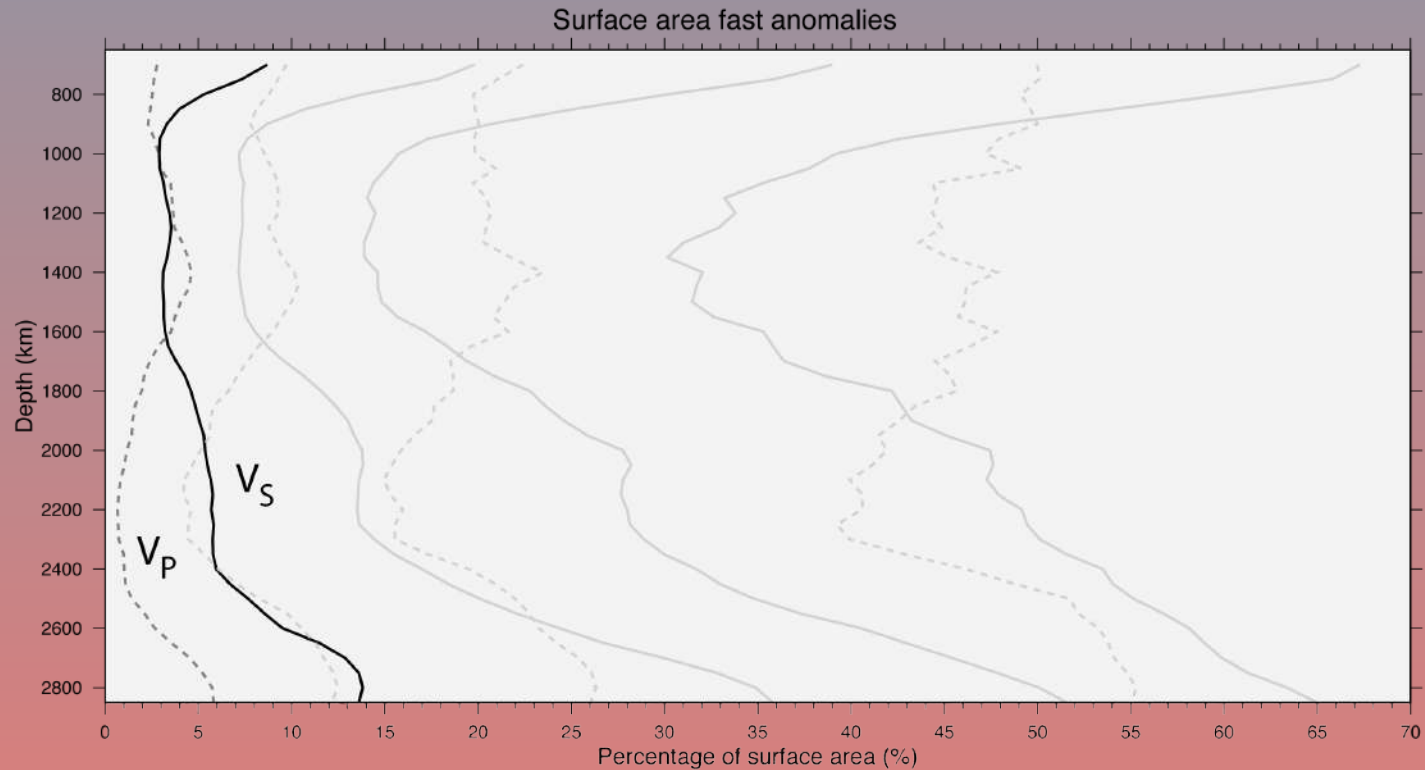


1400 km

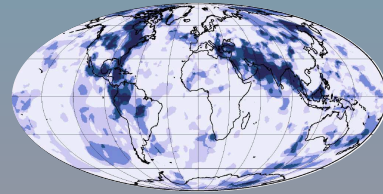
Surface area calculations



1400 km



Change in coverage



a. Fast anomalies ($+1\sigma$)

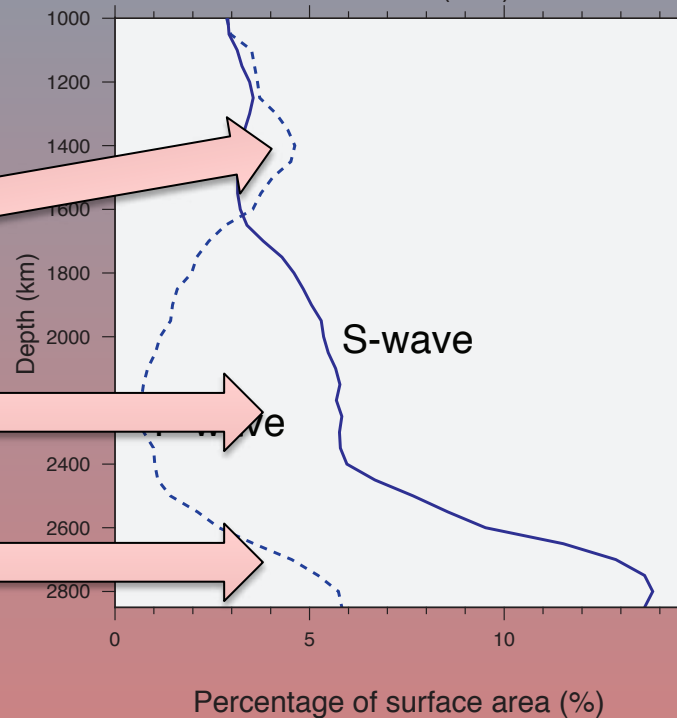
Fast anomalies

- Clear mid-mantle decorrelation

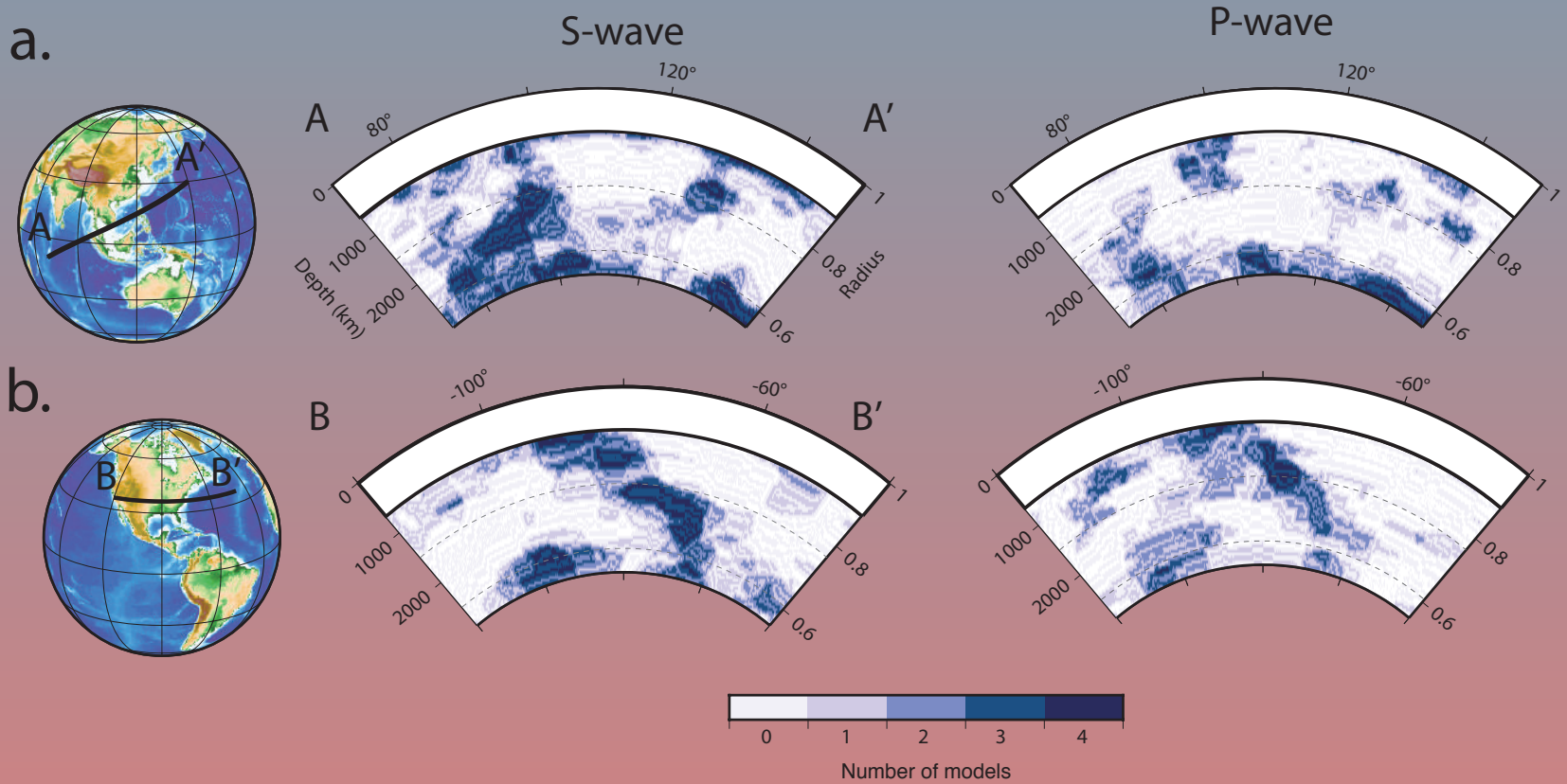
Onset of decorrelation below 1400 km

Matching again below 2200 km

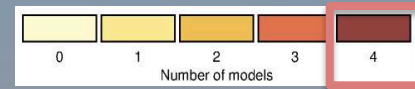
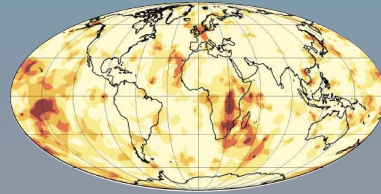
Slab graveyard and LLSVP effect



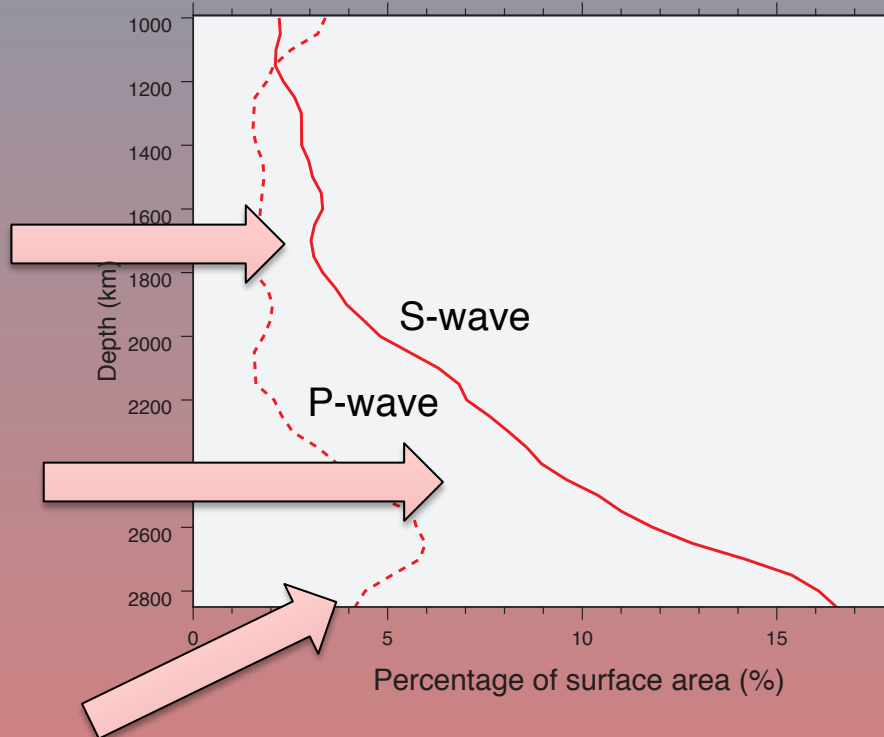
Fast anomalies



Change in coverage



b. Slow anomalies (-1σ)



Onset of decorrelation
~1700 km

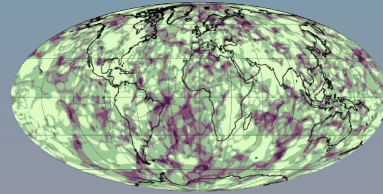
Slab graveyard
and LLSVP
effect

Post-
perovskite(?)

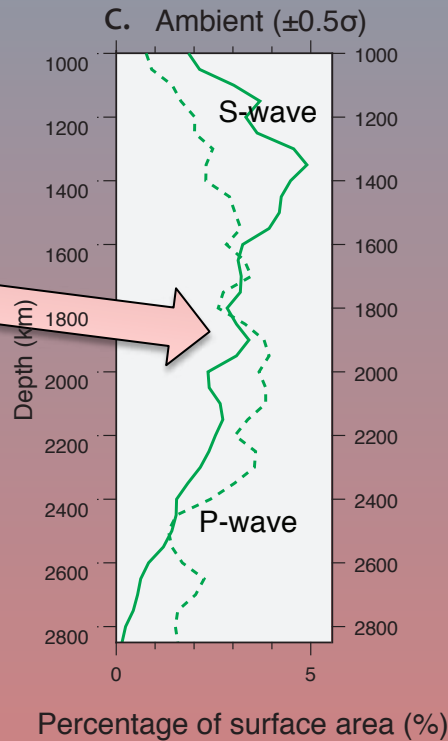
Slow anomalies

- Deeper mid-mantle decorrelation
- LLSVP effects

Change in coverage



No clear
decorrelation



Ambient domain

- No clear signal

Different tomography combos

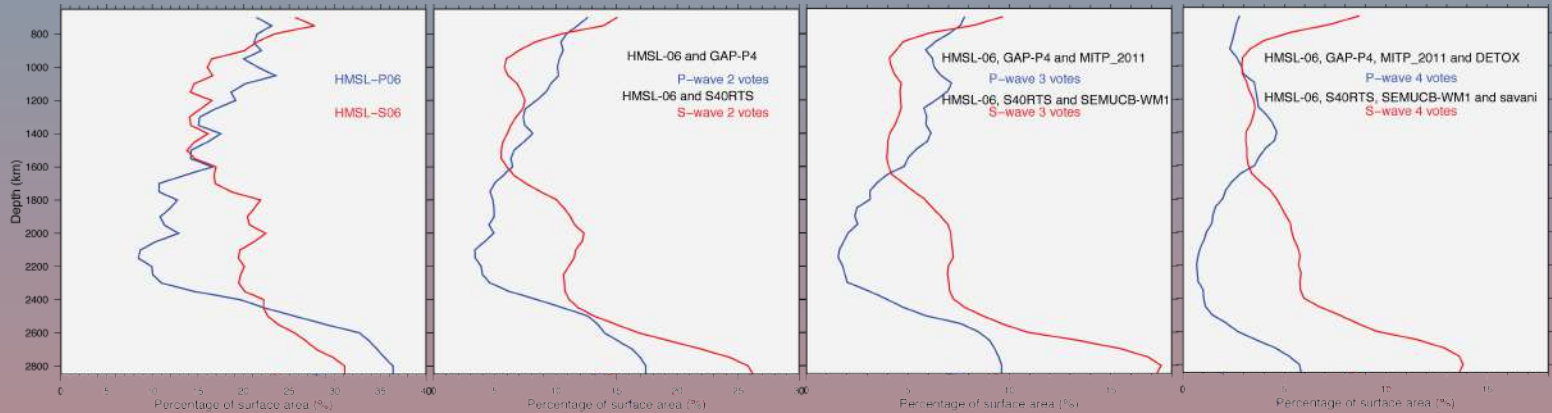
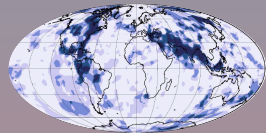
1 model

2 models

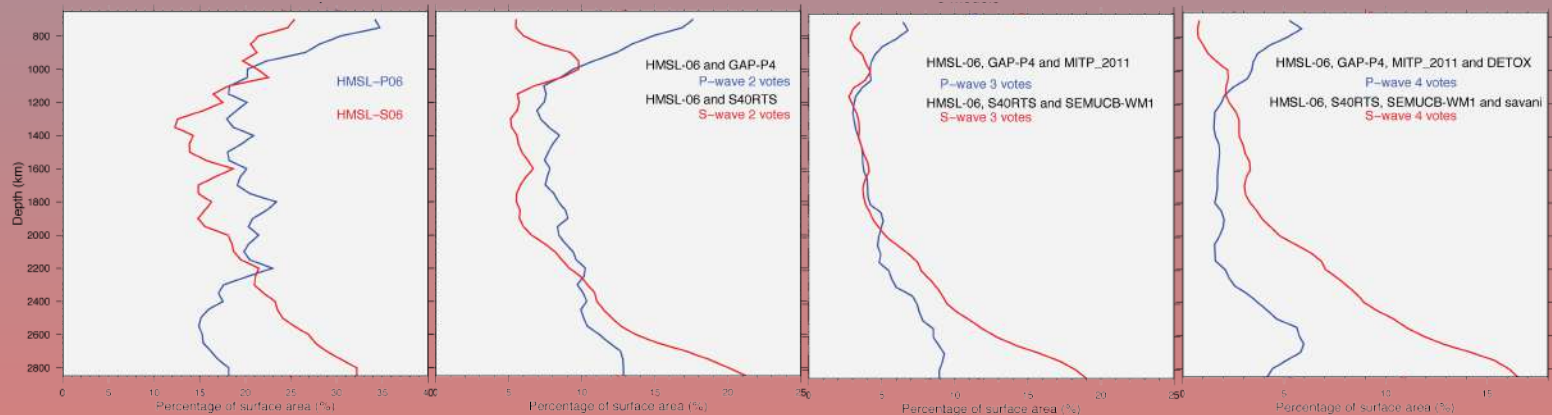
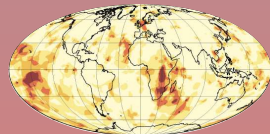
3 models

4 models

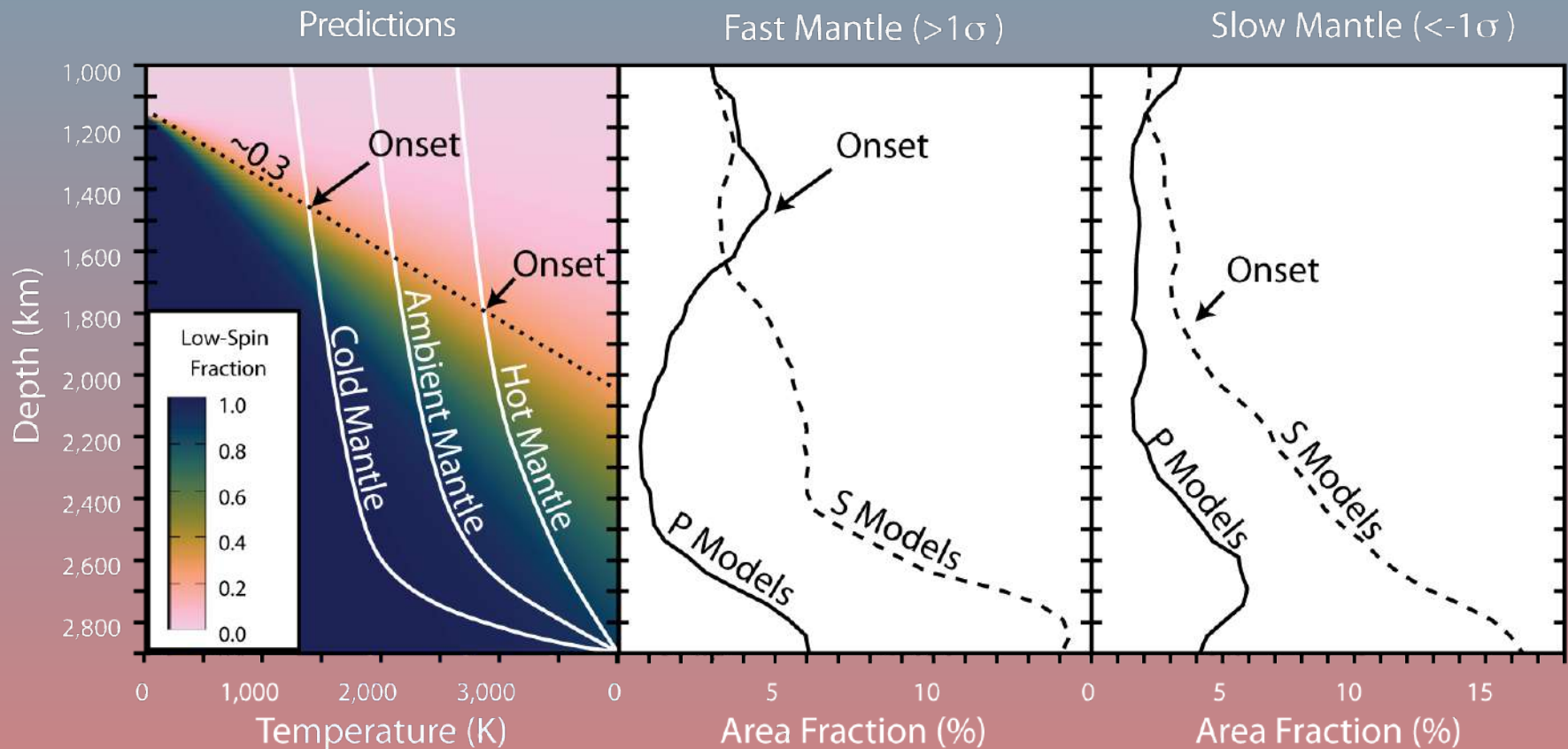
Fast anomalies



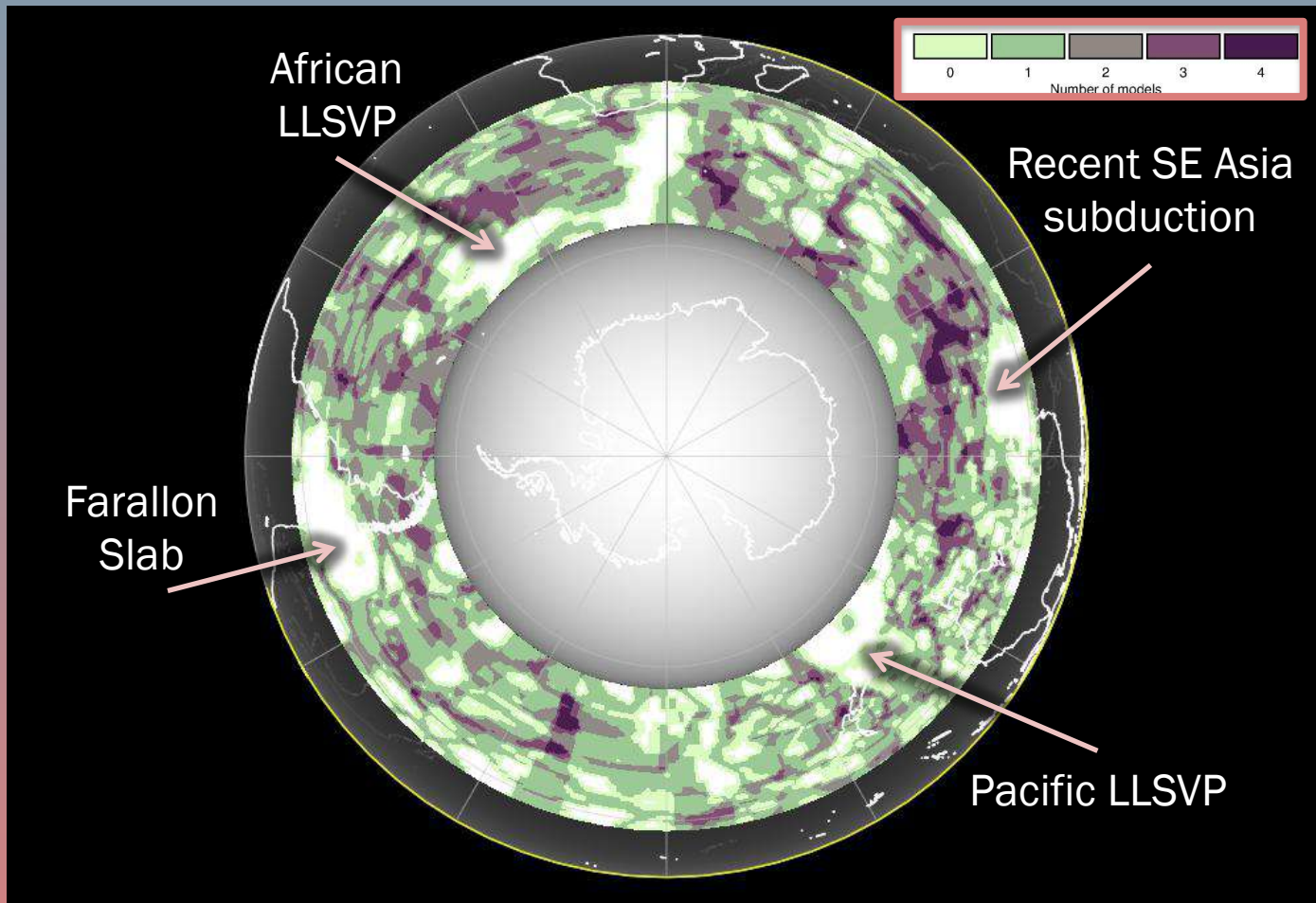
Slow anomalies



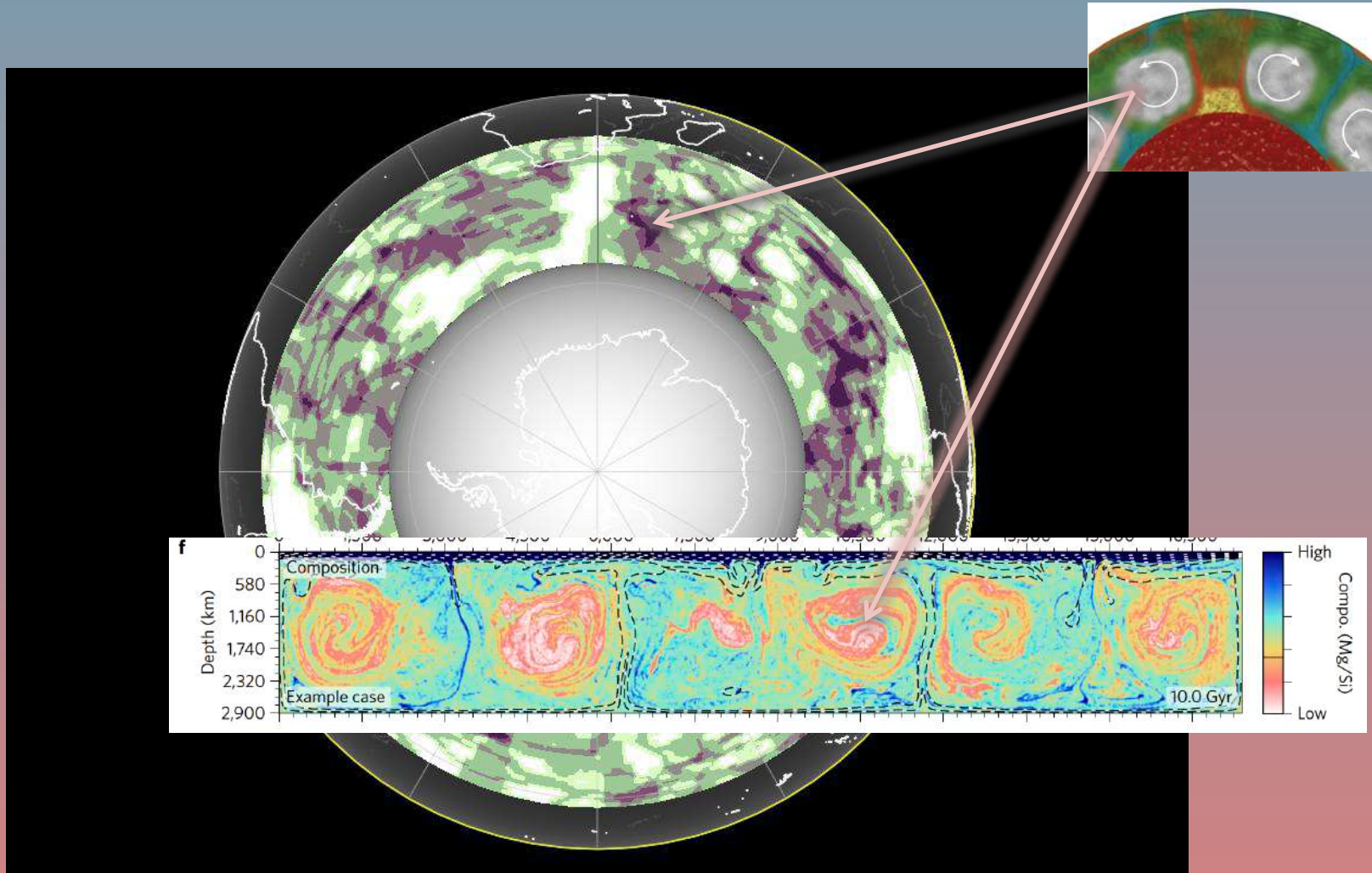
Change in coverage



Ambient mapping



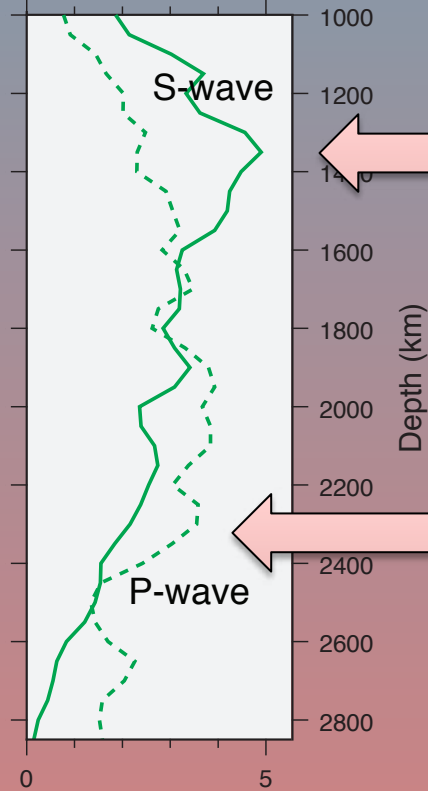
Ambient mapping



BEAMS (Bm-enriched ambient mantle structures) model; Ballmer et al (2015, 2017)

Ambient mapping

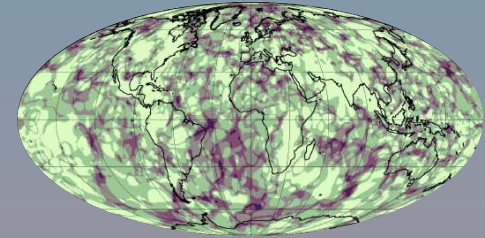
C. Ambient ($\pm 0.5\sigma$)



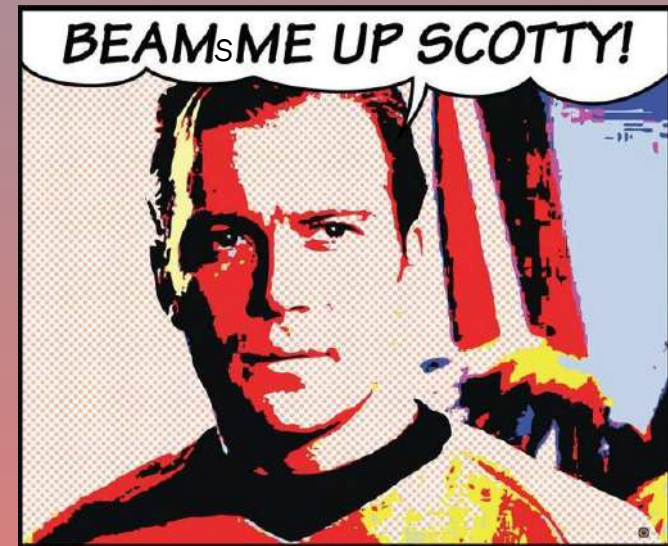
Top of
BEAMS?



Bottom of
BEAMS?



SiO_2 rich, not readily mixed,
rheologically strong,
neutrally buoyant



EGU GD Blog

Weekly blog posts
(Wednesdays)

Looking for guest authors!

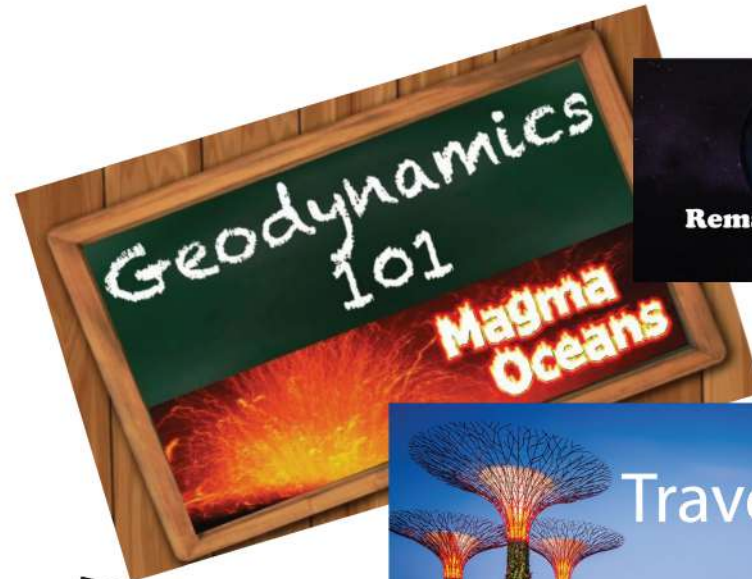
Speak to:

Diogo Lorenço
Antoine Rozel
Anna Gülcher
Anne Glerum
Tobias Meier



Looking for guest contributions

<https://blogs.egu.eu/divisions/gd/>



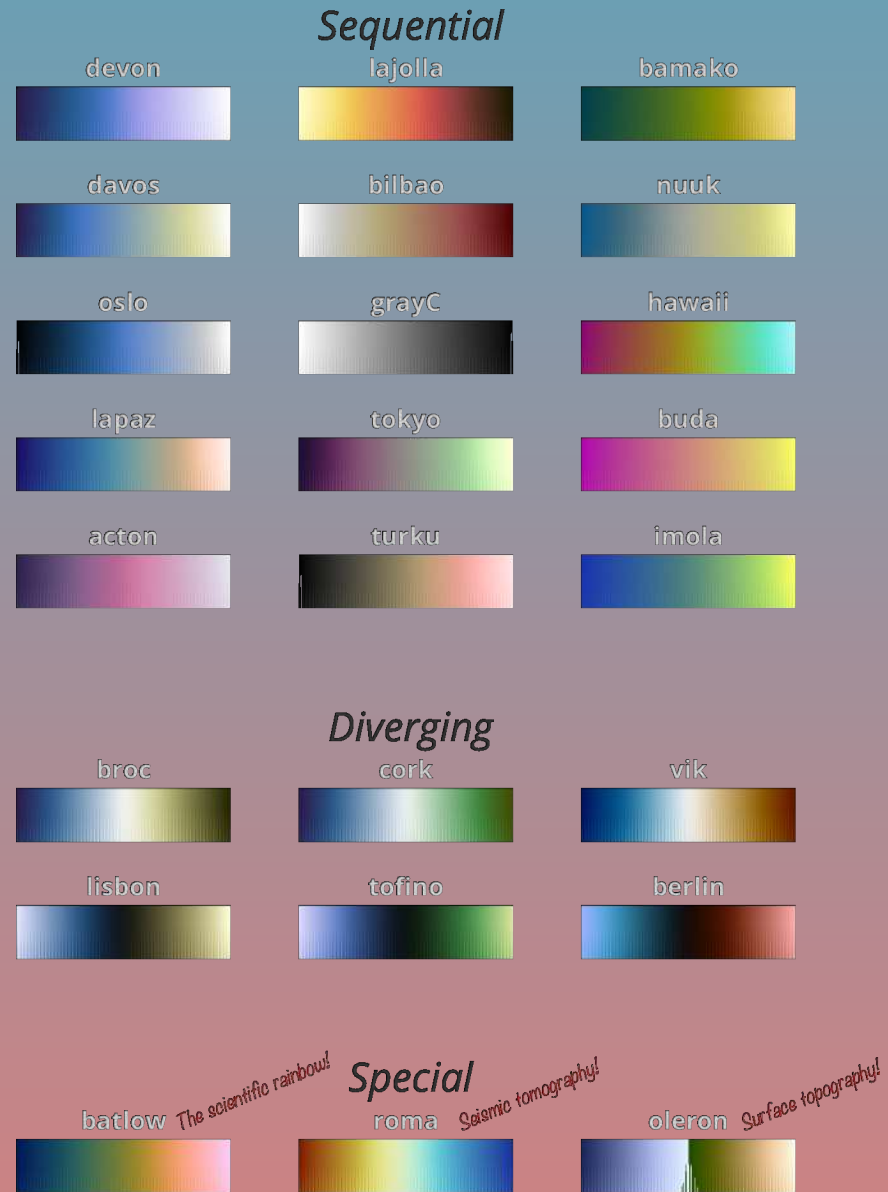
*News and Views
Conference Reporting
Early Career Events
... and more!*

Scientific Colour Maps



www.fabiocrameri.ch/colourmaps.php

Scientific colour-maps



Conclusions



Changes in volume necessitate changes in bulk modulus



Spin transition can be detected by evaluating multiple V_p and V_s tomography models

- Below ~ 1400 km in fast/cold regions
- Below ~ 1700 km in slow/warm regions



Ambient mantle likely contains little F_p – SiO_2 enriched

- Consistent with the BEAMS model

